JOURNAL OF INFORMATION SCIENCE AND ENGINEERING 35, 1223-1248 (2019)
DOI: 10.6688/JISE.201911_35(6).0004

S-DF Cooperative Communication System Over Time Selective Fading Channels

RAVI SHANKAR AND R. K. MISHRA
Department of Electronic and Communication Engineering
National Institute of Technology
Patna, Bihar, 800005 India
E-mail: {ravishankar.ece14; ritesh}@nitp.ac.in

This paper investigates the impact of node mobility and imperfect channel state information (CSI) on the end-to-end performance of a selective decode-and-forward (S-DF) based multiple-input multiple-output (MIMO) space-time block-code (STBC) cooperative wireless system. A closed form expression is derived for the per-block average pair-wise error probability (PEP) for several configurations in terms of number of phases, hops and relays over time selective Rayleigh fading channel, with best relay selection (BRS) and path selection (PS). Further, a framework is developed for deriving the diversity order (DO) for each configuration. Results show that when both destination node (DN) and source node (SN) are immobile, system performance does not encounter asymptotic error floor although relay node (RN) is mobile. Although with mobile RN, the movement of either the DN or the SN critically affects system performance by asymptotic error floors. System performance is analyzed for both equal power and optimal power scenario and the results show that system performance improves with optimal power. Simulation results are in close agreement with the analytical results at high signal to noise ratio (SNR) regimes.

Keywords: channel state information, optimal power allocation, selective decode and forward, node mobility, relay selection, path selection, pairwise error probability

1. INTRODUCTION

Cooperative wireless communication [1] significantly improves the data transfer rate and improving the bit error rate (BER) through the additional cooperation diversity inherent in such wireless systems [2]. Cooperative communication is the natural choice for 5th Generation [2] wireless communication system and has already employed in the 4th Generation system along with MIMO [3]. Along these lines, it is noteworthy to examine the performance of the relay assisted communication system considering practical conditions like imperfect CSI and outdated CSI, Doppler effects, time-selective fading channel, mobile nodes and so forth. In recent times, these problems have been intensively examined in the works [4, 5, 7, 14-16]. In [4], the authors investigated the effect of imperfect CSI at the RN on the end-to-end system performance. Variable gain Amplify and Forward (AF) network is considered in this work. In [5], symbol error rate (SER) performance analysis has been considered for multiple relay S-DF relaying network, assuming time-varying channel, due to the Doppler spread effect, and using the pilot-symbol-assisted modulation (PSAM) technique for their modeling.

Relay selection that instructs a subset of RNs in the relaying network to forward

Received April 7, 2018; revised June 22, 2018; accepted August 16, 2018.
Communicated by Xiaohong Jiang.

symbol has been considered as an effective technique to enhance the end-to-end reliability of the relaying network [6]. In [7], the authors employed the 1st order autoregressive process (AR1) to model the time-varying fading channel links of orthogonal STBC-AF network, considering the BRS and conventional cooperation protocols a closed form SER expression is derived. In this work, CSI is not necessary at the RNs and at the DN. For decoding purpose, differential coherent detection is considered at the DN. In [8], the authors investigated the multiple hop AF and decode-and-forward (DF) relaying network with considering the BRS, which improves the end-to-end system performance of the relaying network by reducing the system complexity. However, in this paper authors have not considered the time-selective fading channel. In [9], the authors have investigated the end-to-end error performance of multiple relay hybrid incremental DF cooperation system with an opportunistic relay selection under Rayleigh fading channels. Simulation outcomes reveal that system performance improves by increasing RNs.

In [10], the authors investigated the PS based relaying network, in which the RN selects either the direct source-to-destination (SD) or source-relay-destination (SRD) fading link for data transmission. This work proposes a generalized network, which is appropriate for numerous physical layer techniques. In [11], the authors analyzed single relay MIMO S-DF relaying network in which the SN, RN and DN are employed with N_S, N_R and N_D antennas, respectively. The authors have proposed joint antenna and PS technique, which jointly chooses the single transmit and receive antenna pairs, along with the selection of either cooperation mode SRD transmission or direct mode SD transmission. The authors have used maximum-minimum-maximum criterion of instantaneous SNR. A closed-form bit error rate (BER) expression for the S-DF MIMO system with M-PSK modulation is derived. But this work has not considered time selective fading and node mobility. In [12], the authors employed a maximum-minimum technique for PS towards S-DF relaying network and present the associated SER performance over time invariant independent and identically distributed (i.i.d.) Rayleigh channels. But this work considers only single antenna and cannot be employed to MIMO scenarios, which is essential for 5th generation wireless communication systems. In [13], the authors investigated multiple hop cooperative communication system considering path selection and node mobility. In this work, two path consistency based path selection strategy has been proposed for multiple hop cooperative communication. In [14], the authors analyzed the outage probability for the path selection based MIMO beamforming relaying network considering imperfect CSI and moving nodes. But this work is limited to the single relay cooperation system and is not applicable for multiple relay scenarios.

However to the best of our knowledge, above, works have not addressed the end-to-end performance analysis of BRS and PS based S-DF [16-18] relaying network considering both node mobility and imperfect CSI. In this work, we consider modified harmonic mean function (HMF) of its SR and RD instantaneous channel gains as an appropriate metric for relay selection. We calculate the ratio between the SD channel gain and MHM and comparing it with cooperation threshold. If this ratio is greater (less) than the cooperation threshold, then cooperation mode SRD transmission will take place. Otherwise, the source sends signal directly to destination, *i.e.* SD mode of transmission will take place.

The organization of the paper is as follows. The system model is given in Section 2. In Section 3, a closed form expression is derived for the per-block average pair-wise error probability (PEP) for several configurations in terms of number of phases, hops and relays over time-selective Rayleigh fading channel, with BRS. In Section 4, PEP performance for PS based S-DF protocol is given. Section 5 analyses the effect of node mobility on the PEP performance along with asymptotic floor. Simulation results and discussion are pro-vided in Section 6 and finally conclusions are given in Section 7.

2. SYSTEM MODEL

2.1 Channel Model

We assume all the fading channel links are time-selective in nature. Also, we assume links will not vary for every STBC codeword matrix. It differs in a time-selective way from one STBC codeword to another STBC codeword within a block. The time selective MIMO fading links can be modeled using AR1 as [7, 14-17, 19],

$$\mathbb{Z}_i(p) = \upsilon_i \mathbb{Z}_i(p-1) + \sqrt{1-\upsilon_i^2}\, E_i(p);\ i \in \{SD, SR, RD\}. \tag{1}$$

Where the terms υ_{SD}, υ_{SR} and υ_{RD} denote the correlation coefficients for the SD so source-to-relay (SR) and relay-to-destination (RD) links respectively. These correlation coefficients can be evaluated using Jakes model [7, 14-17, 19] as, $\upsilon = J_0(2\prod f_c v_p/R_S c)$, where v_p is the relative velocity, $R_S = 1/T_S$ is the symbol transmission rate, T_S denotes the signal time, c denotes the light speed, f_c is the carrier frequency and $J_0(\cdot)$ denotes the zeroth-order Bessel function of the 1st kind [14]. The random process $E_i(p)$ is a zero mean circular shift complex Gaussian noise (ZMCSCG) {*i.e.*, $\sim \mathbb{CN}(0, \sigma_{e_i}^2)$} and denotes the time-varying component of the associated link [15]. In system model, we consider that the DN employs low complexity maximal ratio combiner (MRC) receiver [2]. However, it is difficult to get instantaneous CSI corresponding to the transmission of every STBC codeword due to the time-selective nature of the fading links. Hence, similar to works [7, 14-17, 19] we assume imperfect CSI at the RN and DN. The estimated channel matrices for RD, SR and SD links can be written as [19], $\mathbb{Z}_{RD}(1) = \mathbb{Z}_{RD}(1) + \mathbb{Z}_{\in_{RD}}(1)$, $\mathbb{Z}_{SR}(1) = \mathbb{Z}_{SR}(1) + \mathbb{Z}_{\in_{SR}}(1)$ and $\hat{\mathbb{Z}}_{SD}(1) = \mathbb{Z}_{SD}(1) + \mathbb{Z}_{\in_{SD}}(1)$, respectively, estimated at the beginning of each block and in this way used to detect each STBC codeword $X_S(p)$, $1 \le p \le N_b$ in the consequent block. The MIMO channel matrices $\mathbb{Z}_{SR}(1) \in \mathbb{C}^{N\times N}$, $\mathbb{Z}_{RD}(1) \in \mathbb{C}^{N_D\times N}$ and $\mathbb{Z}_{SD}(1) \in \mathbb{C}^{N_D\times N}$ are comprised of entries $h_{l,m}^{(SR)}(p)$, $h_{n,l}^{(RD)}(p)$ and $h_{n,m}^{(SD)}(p)$ which are ZMCSCG with variance $\delta_{SR}^2, \delta_{RD}^2$ and δ_{SD}^2 respectively. The channel error matrices $\mathbb{Z}_{\in_{RS}}(1)$, $\mathbb{Z}_{\in_{SD}}(1)$ and $\mathbb{Z}_{\in_{RD}}(1)$ comprise of entries, which are ZMCSCG with variance $\sigma_{\in_{SR}}^2$, $\sigma_{\in_{SR}}^2$, and $\sigma_{\in_{SR}}^2$ respectively. By using Eq. (1), $\mathbb{Z}_{\in_{SD}}(p)$ can be modeled as [7, 14-17, 19],

$$\mathbb{Z}_{SD}(p) = \upsilon_{SD}^{p-1}\, \hat{\mathbb{Z}}_{SD}(1) - \upsilon_{SD}^{p-1}\, \mathbb{Z}_{\in_{SD}}(1) + \sqrt{1-\upsilon_{SD}^2} \sum_{i=1}^{p-1} v_{SD}^{p-i-1}\, E_{SD}(i). \tag{2}$$

2.2 Signal Model

Consider multiple hop multiple relay multiple phase S-DF cooperative communication system employing BRS strategy with N_R, N_D and N_S are the number of antennas employed at the RN, DN and SN respectively. In order to keep the data rate of the SR link same as that of the RD link, we employ the same STBC at the RN and SN. This also means that $N_R = N_S = N$ [14-22]. Schematic representation of BRS based S-DF relaying scheme is given in Fig. 1 (a).

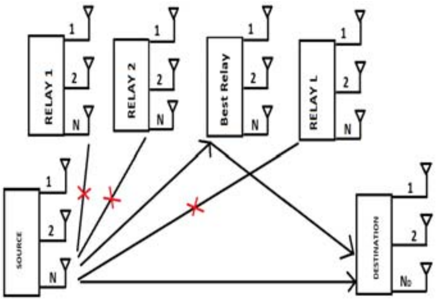

Fig. 1. (a) Schematic representation of BRS based S-DF cooperative communication protocol.

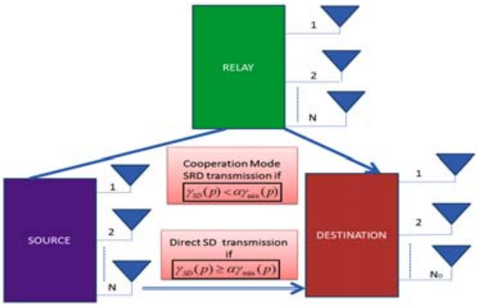

Fig. 1. (b) Schematic representation of path selection based single relay S-DF cooperative communication protocol.

The BRS based S-DF relaying scheme can be described as follows. Let $C = \{X_j(p)\}$ denotes the STBC codeword set, where each codeword of the set C is expressed as, $X_j(p) \in \mathbb{C}^{N \times T_S}$ and $1 \leq j \leq |C|$, where $|C|$ denotes the cardinality of the codeword set C [14-16, 19]. The fundamental idea of the proposed S-DF relaying technique relies upon choosing best RN among the L RNs to cooperate with the SN, in the event that it needs cooperation. The received symbol block at the DN in case of direct SD transmission mode is modeled as [7, 14-17],

$$Y_{SD}[p] = \sqrt{P / NR_C}\, \upsilon_{SD}^{p-1} \hat{\mathbb{Z}}_{SD}[1] X_S[p] + \tilde{W}_{SD}[p]. \tag{3}$$

Where P, N and R_C denote the total available power budget, number of antennas at the SN and coding rate respectively. For cooperation mode, the received symbol blocks at the RN and DN can be modeled as [15, 20],

$$Y_{SR}[p] = \sqrt{P_1 / NR_C}\, \upsilon_{SR}^{p-1} (\mathbb{Z}_{SR}[1] + \mathbb{Z}_{\in_{SR}}[1]) X_S[p] + \tilde{W}_{SR}[p], \tag{4}$$

$$Y_{RD}[p] = \sqrt{\tilde{P}_2 / NR_C}\, \upsilon_{RD}^{p-1} (\mathbb{Z}_{RD}[1] + \mathbb{Z}_{\in_{RD}}[1]) X_S[p] + \tilde{W}_{RD}[p]. \tag{5}$$

Where, $\begin{cases} \tilde{P}_2 = P_2; & \text{if relay } L \text{ decodes the symbol correcly} \\ \tilde{P}_2 = 0; & \text{if relay } L \text{ decodes the symbol incorrecly} \end{cases}.$

In Eq. (4), P_2 denotes the optimal relay power for source-best relay-destination transmission. The noise matrix $\tilde{W}_{SD}[p]$, $\tilde{W}_{SR}[p]$ and $\tilde{W}_{RD}[p]$ are comprised of noise terms emerging because of the moving nodes and imperfect CSI respectively [15, 16, 19]. The effective noise variances η_{SD}, η_{SR} and η_{RD} for SD, SR and RD links can be modeled as [7, 14-16, 19],

$$\eta_{SD} = N_0 + P(NR_C)^{-1}\upsilon_{SD}^{2(p-1)}N_a\sigma^2_{\in SD} + P(NR_C)^{-1}\left(1-\upsilon_{SD}^{2(p-1)}\right)N_a\sigma^2_{eSD},$$
$$\eta_{SR} = N_0 + P_1(NR_C)^{-1}\upsilon_{SR}^{2(p-1)}N_a\sigma^2_{\in SR} + P_1(NR_C)^{-1}\left(1-\upsilon_{SR}^{2(p-1)}\right)N_a\sigma^2_{eSR},$$
$$\eta_{RD} = N_0 + \tilde{P}_2(NR_C)^{-1}\upsilon_{RD}^{2(p-1)}N_a\sigma^2_{\in RD} + \tilde{P}_2(NR_C)^{-1}\left(1-\upsilon_{RD}^{2(p-1)}\right)N_a\sigma^2_{eRD}, \tag{6}$$

respectively. Where N_a denotes the number of non-zero M-PSK symbols transmitted per codeword [16]. The advantage of using STBC code-word is that, it orthogonalizes the vector channel into a constant scalar channel by creating virtual parallel paths [15, 16]. The effective instantaneous SNR $\gamma_{SD}(p)$, $\gamma_{SR}(p)$, and $\gamma_{RD}(p)$ for the SD, SR and RD fading links respectively can be modeled as [14-19, 22],

$$\gamma_{SD}(p) = \frac{P\upsilon_{SD}^{2(p-1)}\left\|\hat{\mathbb{Z}}_{SD}(1)(X_S(p)-X_j(p))\right\|_F^2}{2NR_C\eta_{SD}} = \frac{P\upsilon_{SD}^{2(p-1)}\sum_{n=1}^{N}\lambda_{1n}^2\sum_{\tilde{l}=1}^{N}\left|\tilde{h}_{\tilde{l},n}^{SD}\right|^2}{2NR_C\eta_{SD}},$$
$$\gamma_{SR}(p) = \frac{P_1\upsilon_{SR}^{2(p-1)}\left\|\hat{\mathbb{Z}}_{SR}(1)(X_S(p)-X_j(p))\right\|_F^2}{2NR_C\eta_{SR}} = \frac{P_1\upsilon_{SR}^{2(p-1)}\sum_{n=1}^{N}\lambda_{ln}^2\sum_{\tilde{n}=1}^{N}\left|\tilde{h}_{\tilde{n},n}^{(SR)}(1)\right|^2}{2NR_C\eta_{SR}},$$
$$\gamma_{RD}(p) = \frac{\tilde{P}_2\upsilon_{RD}^{2(p-1)}\left\|\hat{\mathbb{Z}}_{RD}(1)(X_S(p)-X_j(p))\right\|_F^2}{2NR_C\eta_{RD}} = \frac{\tilde{P}_2\upsilon_{RD}^{2(p-1)}\sum_{n=1}^{N}\lambda_{jn}^2\sum_{l=1}^{N_D}\left|\tilde{h}_{l,n}^{(RD)}(1)\right|^2}{2NR_C\eta_{RD}}. \tag{7}$$

The effective SNRs $\gamma_{SD}(p)$, $\gamma_{SR}(p)$ and $\gamma_{RD}(p)$ are Gamma distributed in nature, having a cumulative distribution function (CDF) and probability distribution function (PDF) and is modeled as [14-17, 19, 22],

$$F_\gamma(t) = \gamma(\Theta, \Lambda t)\{\Gamma(\Theta)\}^{-1}, f_r(t) = \wedge^{\Theta}t^{\Theta-1}\{\Gamma(\Theta)\}^{-1}e^{-\Lambda t}. \tag{8}$$

Where $\gamma(\cdot,\cdot)$ denotes the lower incomplete Gamma function [14-17, 19, 22] and the quantities (Θ, Λ) will be equal to $[NN_D, \{C_{SD}(p)\tilde{\delta}^2_{SD}\}^{-1}]$, $[N^2, \{C_{SD}(p)\tilde{\delta}^2_{SR}\}^{-1}]$ and $[NN_D, \{C_{RD}(p)\tilde{\delta}^2_{RD}\}^{-1}]$ for the SR, SD, and RD SNR's respectively [14-17, 19, 22]. Where $C_{SD}(p)$, $C_{SR}(p)$ and $C_{RD}(p)$ are given as [14-17, 19, 22],

$$C_{SD}(p) = \left\{\bar{\gamma}_{SD}\upsilon_{SD}^{2(p-1)}(NR_C)^{-1}\right\}\left\{1+\bar{\gamma}_{SD}(NR_C)^{-1}\upsilon_{SD}^{2(p-1)}\tilde{\sigma}^2_{\in_{SD}} + \bar{\gamma}_{SD}(NR_C)^{-1}\left(1-\upsilon_{SD}^{2(p-1)}\right)\tilde{\sigma}^2_{e_{SD}}\right\}^{-1},$$
$$C_{SR}(p) = \left\{\bar{\gamma}_{SR}\upsilon_{SR}^{2(p-1)}(NR_C)^{-1}\right\}\left\{1+\bar{\gamma}_{SR}(NR_C)^{-1}\upsilon_{SR}^{2(p-1)}\tilde{\sigma}^2_{\in_{SR}} + \bar{\gamma}_{SR}(NR_C)^{-1}\left(1-\upsilon_{SR}^{2(p-1)}\right)\tilde{\sigma}^2_{e_{SR}}\right\}^{-1},$$
$$C_{RD}(p) = \left\{\bar{\gamma}_{RD}\upsilon_{RD}^{2(p-1)}(NR_C)^{-1}\right\}\left\{1+\bar{\gamma}_{RD}(NR_C)^{-1}\upsilon_{RD}^{2(p-1)}\tilde{\sigma}^2_{\in_{RD}} + \bar{\gamma}_{RD}(NR_C)^{-1}\left(1-\upsilon_{RD}^{2(p-1)}\right)\tilde{\sigma}^2_{e_{RD}}\right\}^{-1}, \tag{9}$$

respectively. The quantities $\tilde{\delta}^2_{\in SR}$, $\tilde{\delta}^2_{eSR}$, $\tilde{\delta}^2_{\in RD}$ and $\tilde{\delta}^2_{eRD}$ are equivalent to $N_a\sigma^2_{\in SR}$, $N_a\sigma^2_{eSR}$, $N_a\sigma^2_{\in RD}$ and $N_a\sigma^2_{eRD}$ respectively [19]. The parameters $\bar{\gamma}_{SR}$, $\bar{\gamma}_{RD}$ and $\bar{\gamma}_{SD}$ are given as $\bar{\gamma}_{SR} = P_1/N_0$, $\bar{\gamma}_{RD} = P_2/N_0$ and $\bar{\gamma}_{SD} = P/N_0$ respectively. The quantities $\tilde{\delta}^2_{SR}$, $\tilde{\delta}^2_{SD}$ and $\tilde{\delta}^2_{RD}$ are defined as, $\tilde{\delta}^2_{SR} = \delta^2_{SR} + \sigma^2_{\in SR}$, $\tilde{\delta}^2_{SD} = \delta^2_{SD} + \sigma^2_{\in SD}$ and $\tilde{\delta}^2_{RD} = \delta^2_{RD} + \sigma^2_{\in RD}$ respectively [14-16]. The terms $\tilde{\delta}^2_{\in SD}$ and $\tilde{\sigma}^2_{eSD}$ are equivalent to $N_a\sigma^2_{\in SD}$ and $N_a\sigma^2_{eSD}$ respectively, λ_{l1}, λ_{l2}, …, λ_{lN}

represents the singular values (SVs) obtained after performing the singular value decomposition (SVD) [17] of the STBC codeword difference $X_S(p) - X_j(p), \tilde{h}_{\tilde{l},n}^{SD}$ represents the $(\tilde{l}, n)$ coefficient of the matrix $\tilde{\mathbb{Z}}_{SD}(1) = \hat{\mathbb{Z}}_{SD}(1)U_j$ for $1 \le \tilde{l}, n \le N$ and $U_j \in \mathbb{C}^{N\times N}$ is a unitary matrix, *i.e.*, $U_jU = UU_j = I_{N\times N}$ and for orthogonal-STBC we take $\lambda_{l1} = \lambda_{l2} = \ldots = \lambda_{lN} = \lambda$ [16-19].

2.3 Relay Selection Algorithm

Let metric β_i be defined as the HMF, μ_H of its SR and RD link variances as [20],

$$\beta_i = \mu_H\{q_1\beta_{R_iD}, q_2\beta_{SR_i}\} = 2q_1q_2\beta_{R_iD}\beta_{SR_i}\{q_1\beta_{R_iD} + q_2\beta_{SR_i}\}^{-1}; i = 1, 2, \ldots, L. \tag{10}$$

Where $\beta_{SR_i} = \left|\tilde{h}_{\tilde{n},n}^{(SR_i)}(1)\right|^2$, $\beta_{R_iD} = \left|\tilde{h}_{\tilde{l},n}^{(R_iD)}(1)\right|^2$, $q_1 = A^2/g^2$, $q_2 = B/g(1-g)$, $A = (M-1)(2M)^{-1} + \sin(2pi/M)(4pi)^{-1}$, $B = 3(M-1)(8M)^{-1} + \sin(2pi/M)(4pi)^{-1} - \sin(4pi/M)(32pi)^{-1}$ and $g \triangleq P_1/P$ denotes the power ratio, P_1 and P denote the source and total power respectively in the case of cooperation mode. Let $\beta_{\max}$ denotes the optimal RN metric, which is expressed as [20],

$$\beta_{\max} = \max\{\beta_1, \beta_1, \ldots, \beta_L\}. \tag{11}$$

In the 1st phase of the signal transmission, the SN estimates the ratio $\beta_{SD}/\beta_{\max}$ and compares it with cooperation threshold α. Where β_{SD} denotes SD path gain. If $\beta_{SD} \ge \alpha\beta_{\max}$, then direct SD transmission mode will take place. If $\beta_{SD} \le \alpha\beta_{\max}$, then cooperation will take place. In this case SN will choose the optimal relay among the L relay nodes.

3. PERFORMANCE ANALYSIS

3.1 PEP Analysis

For analysis purposes, we consider orthogonal-STBC codeword. We derive the average PEP probability of direct SD transmission and source-best relay-destination modes of transmission of S-DF relaying scenario. Then, these derived expressions are used to derive the average PEP upper bound expression for S-DF protocol. The CDF of β_i for $i = 1, 2, \ldots, L$ is expressed as [20],

$$P_{\beta_i}(\beta_i) = 1 - \beta_i(t_{1,i})^{-1}\exp\{-t_{2,i}\beta_i/2\}K_1(\beta_i(t_{1,i})^{-1}). \tag{12}$$

Where $t_{1,i} = (q_1q_2\delta^2_{SR_i}\delta^2_{R_iD})^{0.50}$, $t_{2,i} = (q_2\delta^2_{SR_i})^{-1} + (q_1\delta^2_{R_iD})^{-1}$ and $K_1(x)$ denotes the first-order modified Bessel functions of the second kind [1, 2]. The CDF of $\beta_{\max}$ can be expressed as [1, 2, 20], $P_{\beta_{\max}}(\beta) = P_r(\beta_1 \le \beta, \ldots, \beta_L \le \beta) = \prod_{i=1}^{L} P_{\beta_i}(\beta)$ and the PDF of $\beta_{\max}$ can be written [1-5, 17-20],

$$p_{\beta_{\max}}(\beta) = \frac{\partial P_{\beta_{\max}}(\beta)}{\partial\beta} \approx \sum_{j=1}^{L} p_{\beta_j}(\beta)\left(\prod_{i=1, i\ne j}^{L}\left(1-\exp\left(-0.50t_{2i}\beta\right)\right)\right). \tag{13}$$

Where $p_{\beta_j}(\cdot)$ is the PDF of β_j. We apply an approximation $K_1(x) \approx x^{-1}$ [20] in Eq. (13). For simplicity, we consider symmetric links where all the RNs have the same SR and RD channel gains, *i.e.*, $\delta^2_{SR_i} = \delta^2_{SR}$ and $\delta^2_{R_iD} = \delta^2_{RD}$ for $i = 1, 2, \ldots, L$.

Let $t_1 = \{q_1 q_2 \delta^2_{SR} \delta^2_{RD}\}^{-1}$ and $t_2 = (q_2 \delta^2_{SR}) + (q_1 \delta^2_{RD})^{-1}$. The CDF and PDF of $\beta_{\max}$ can be modeled as [1, 2, 19, 20],

$$P_{\beta_{\max}}(\beta) = \{1 - \beta t_1^{-1} \exp(-0.50 t_2 \beta) K_1(\beta t_1^{-1})\}^L,\ p_{\beta_{\max}}(\beta) = L\{1 - \beta t_1^{-1} \exp(-0.50 t_2 \beta) K_1(\beta t_1^{-1})\}^{L-1} p_{\beta_m}(\beta), \tag{14}$$

respectively, where $p_{\beta_m}(\cdot)$ denotes the PDF of β_m [1-5, 20], $\beta_m = \mu_H(q_1\beta_{RD}, q_2\beta_{SR}) \triangleq 2q_1q_2\beta_{SR}\beta_{RD}\{q_1\beta_{RD} + q_2\beta_{SR}\}^{-1}$, modeled in Eq. (15) [20],

$$p_{\beta_m}(\beta_m) = 0.50\beta_m t_1^{-2} \exp(-0.50 t_2 \beta_m)(t_1 t_2 K_1(\beta_m t_1^{-1}) + 2K_0(\beta_m t_1^{-1}))U(\beta_m). \tag{15}$$

Where $\beta_{SR} = \left|\tilde{h}^{(SR)}_{\tilde{n},n}(1)\right|^2$, $\beta_{RD} = \left|\tilde{h}^{(RD)}_{l,n}(1)\right|^2$ and $U(\cdot)$denotes the unit step function. The error probability corresponding to the direct SD transmission error event $\Phi = (\beta_{SD} \geq \alpha\beta_{\max})$ can be expressed as [1-5, 19, 20],

$$P_r(\Phi) = P_r(\beta_{SD} \geq \alpha\beta_{\max}) = \int_0^\infty P_{\beta_{\max}}\left(\beta_{SD}\alpha^{-1}\right) p_{\beta_{SD}}(\beta_{SD}) d\beta_{SD} \tag{16}$$

$$= \sum_{n=0}^{L} \binom{L}{n} (-1)^n \frac{1}{(\alpha t_1)^n \delta^2_{SD}} \int_0^\infty \beta^n_{SD} \exp\left(-\left(\frac{1}{\delta^2_{SD}} + \frac{t_2 n}{2\alpha}\right)\beta_{SD}\right)\left(K_1\left(\frac{\beta_{SD}}{\alpha t_1}\right)\right)^n d\beta_{SD} \approx \sum_{n=0}^{L} \binom{L}{n} (-1)^n \frac{2\alpha}{2\alpha + t_2 n \delta^2_{SD}}.$$

Where we employ approximation $K_1(x) \approx x^{-1}$ in Eq. (16) [20], β_{SD} is an exponential random variable (RV) with average channel gain equal to δ^2_{SD}. The relaying mode error probability corresponding to the error event $\Phi^c = (\beta_{SD} \leq \alpha\beta_{\max})$ is given as, $P_r(\Phi^c) = 1 - P_r(\Phi)$. The average PEP is modeled as [15, 20],

$$P_r(e) = \underbrace{P_r(e/\Phi)P_r(\Phi)}_{\text{Direct SD Transmission Mode}} + \underbrace{P_r(e/\Phi^c)P_r(\Phi^c)}_{\text{Cooperation SRD Transmission Mode}}. \tag{17}$$

Where $P_r(e/\Phi)P_r(\Phi)$ represent the direct SD transmission mode error probability and $P_r(e/\Phi^c)P_r(\Phi^c)$ denotes the SRD transmission mode error probability. The error probability for SD mode can be derived as follows. First, the instantaneous SNR for direct SD transmission is $\gamma_{SD}(p) = \dfrac{P\upsilon_{SD}^{2(p-1)} \sum_{n=1}^{N} \lambda^2_{1n} \sum_{\tilde{l}=1}^{N} \left|\tilde{h}^{SD}_{\tilde{l},n}\right|^2}{2NR_C\eta_{SD}}$. The instantaneous PEP corresponding to the direct SD transmission mode is written as [1, 19, 20],

$$P_r(e/\Phi, \beta_{SD}) = \Psi(\gamma_{SD}(p)) = \frac{1}{pi} \int_0^{\frac{(M-1)pi}{M}} \exp\left(-\left(\sin^2(pi/M)\gamma_{SD}(p)\right)\sin^{-2}(\theta)\right) d\theta. \tag{18}$$

Thus, the average PEP for direct SD transmission mode is modeled as [1, 19, 20],

$$P_r(e/\Phi)P_r(\Phi)=\int_0^{\infty}P_r(e/\Phi,\beta_{SD})P_r(\Phi/\beta_{SD})p_{\beta_{SD}}(\beta_{SD})d\beta_{SD}$$
$$\approx\sum_{n=0}^{L}\binom{L}{n}(-1)^n F_1\left(1+\frac{t_2\delta_{SD}^2 n}{2\alpha}+\frac{bP\delta_{SD}^2\mathrm{A}_1}{\eta_{SD}\sin^2(\theta)}\right)^2. \tag{19}$$

Where $K_1(x)\approx x^{-1}$ in Eq. (19), $F_1(x(\theta))=\frac{1}{pi}\int_0^{\frac{(M-1)pi}{M}}x^{-1}(\theta)d\theta$ [1, 3, 6, 10, 17, 19, 20] and $A_1=0.50\rho_{SD}^{2(p-1)}\lambda^2N^{-1}R_C^{-1}$. For SRD mode, MRC is applied at DN. The instantaneous SNR is written as,

$$\gamma_{SRD}(p)=\frac{P\upsilon_{SD}^{2(p-1)}\sum_{n=1}^{N}\lambda_{1n}^2\sum_{\tilde{l}=1}^{N}\left|\tilde{h}_{\tilde{l},n}^{SD}\right|^2}{2NR_C\eta_{SD}}+\frac{\tilde{P}_2\upsilon_{RD}^{2(p-1)}\sum_{n=1}^{N}\lambda_{jn}^2\sum_{l=1}^{N_D}\left|\tilde{h}_{l,n}^{(RD)}(1)\right|^2}{2NR_C\eta_{RD}}. \tag{20}$$

Considering both scenarios when $\tilde{P}_2=0$ and $\tilde{P}_2=P_2$, the instantaneous PEP of the SRD transmission mode is written as [20],

$$P_r(e/\Phi^c,\beta_{SD},\beta_{SR},\beta_{RD})=\Psi(\gamma_{SRD}(p))\big|_{\tilde{P}_2=0}\Psi(\gamma_{SR}(p))+\Psi(\gamma_{SRD}(p))\big|_{\tilde{P}_2=P_2}(1-\Psi(\gamma_{SR}(p))). \tag{21}$$

Let us consider $P_r(A/\Phi^c,\beta_{SD},\beta_{SR},\beta_{RD})=\Psi(\gamma_{SRD}(p))\Psi(\gamma_{SR}(p))$ and $P_r(B/\Phi^c,\bar{\beta})=\Psi(\gamma_{SRD})$ [1, 2, 19, 20].

$$P_r(A/\Phi^c,\beta_{SD},\beta_{SR},\beta_{RD})=\frac{1}{pi}\int_{\theta_1=0}^{(M-1)M^{-1}pi}\exp\left(-bP_1A_1\eta_{SD}^{-1}\sin^{-2}(\theta)\beta_{SD}\right)\exp\left(-b\tilde{P}_2A_2\eta_{RD}^{-1}\sin^{-2}(\theta)\beta_{RD}\right)d\theta_1$$
$$\times\frac{1}{\Pi}\int_{\theta_2=0}^{(M-1)M^{-1}pi}\exp\left(-bP_1A_3\eta_{SR}^{-1}\sin^{-2}(\theta)\beta_{SR}\right)d\theta_2. \tag{22}$$

Since the value of $P_r(A/\Phi^c,\beta_{SD},\beta_{SR},\beta_{RD})$ can be modeled as shown in Eq. (22), thus,

$$P_r(A/\Phi^c)P_r(\Phi^c)=\int_{\bar{\beta}}P_r(A/\Phi^c,\bar{\beta})P_r(\Phi^c/\bar{\beta})p_{\bar{\beta}}(\bar{\beta})d\bar{\beta}. \tag{23}$$

Where $\bar{\beta}\triangleq[\beta_{SD},\beta_{SR},\beta_{RD}]$, $A_2=0.50\upsilon_{RD}^{2(p-1)}\lambda^2N^{-1}R_C^{-1}$ and $A_3=0.50\upsilon_{SR}^{2(p-1)}\lambda^2N^{-1}R_C^{-1}$. Furthermore,

$$P_r(\Phi^c/\bar{\beta})=P_r\left(\beta_{SD}<\alpha\beta_{\max}/\beta_{SD},\beta_{SR},\beta_{RD}\right)=U(\alpha\beta_{\max}-\beta_{SD}). \tag{24}$$

Substituting Eqs. (22) and (24) into Eq. (23), we get,

$$P_r(A/\Phi^c)P_r(\Phi^c)=\int_{\bar{\beta}}\frac{1}{\Pi^2}\int_{\theta_1=0}^{\frac{(M-1)\Pi}{M}}\int_{\theta_2=0}^{\frac{(M-1)\Pi}{M}}\exp\left(-P_1C(\theta_1)\beta_{SD}\right)\exp\left(-\tilde{P}_2C(\theta_1)\beta_{RD}\right)\exp\left(-C(\theta_2)P_1\beta_{SR}\right)$$
$$\times U\left(\alpha\beta_{\max}-\beta_{SD}\right)p_{\bar{\beta}}(\bar{\beta})d\theta_2 d\theta_1 d\bar{\beta}. \tag{25}$$

Where $C(\theta_1)=\dfrac{b\upsilon_{SD}^{2(p-1)}\lambda^2}{\eta_{SD}\sin^2(\theta)2NR_C}$, $C(\theta_2)=\dfrac{b\upsilon_{SR}^{2(p-1)}\lambda^2}{\eta_{SR}\sin^2(\theta)2NR_C}$. Since β_{SD}, β_{SR} and β_{RD} are statistically independent, thus $p_{\bar{\beta}}(\bar{\beta}) = p_{\beta_{SD}}(\beta_{SD})p_{\beta_{SR}}(\beta_{SR})p_{\beta_{RD}}(\beta_{RD}) = p_{\beta_{SD}}(\beta_{SD})p_{\bar{\beta}_1}(\bar{\beta}_1)$. Where $\bar{\beta}_1 \triangleq [\beta_{SR}, \beta_{RD}]$. Integrating Eq. (25) w.r.t. β_{SD}, we get Eq. (26) [1, 14, 18, 20].

$$P_r(A/\Phi^c)P_r(\Phi^c) = \int_{\bar{\beta}_1}\frac{1}{\Pi^2}\int_{\theta_1=0}^{\frac{(M-1)\Pi}{M}}\int_{\theta_2=0}^{\frac{(M-1)\Pi}{M}}\frac{1-\exp\left(-\left(P_1C(\theta_1)+\frac{1}{\delta_{SD}^2}\right)\alpha\beta_{\max}\right)}{1+P_1C(\theta_1)\delta_{SD}^2}p_{\bar{\beta}_1}(\bar{\beta}_1)$$
$$\times\exp\left(-\left(\tilde{P}_2C(\theta_1)\beta_{RD}+P_1C(\theta_2)\beta_{SR}\right)\right)d\theta_2d\theta_1d\bar{\beta}_1. \tag{26}$$

It is difficult to derive the expression of Eq. (26) for $\beta_{\max}$ expressed in Eq. (11). Thus, we get a PEP upper bound expression via a worst case condition. Replacing β_{SR} and β_{RD} in Eq. (26) by their worst case values in terms of $\beta_{\max}$. Then, we average (26) over $\beta_{\max}$ only. Since, $\beta_{\max} = \mu_H(q_1\beta_{RD}, q_2\beta_{SR})$, we can write $\beta^{1}_{\max} = \{2q_2\beta_{SR}\}^{-1} + \{2q_1\beta_{RD}\}^{-1}$. Then, we replace β_{SR} and β_{RD} by their worst case in terms of $\beta_{\max}$ as, $\beta_{SR} \to \beta_{\max}(2q_2)^{-1}$ and $\beta_{RD} \to \beta_{\max}(2q_1)^{-1}$. Thus, upper bound of Eq. (26) is written as [20],

$$P_r(A/\Phi^c)P_r(\Phi^c) \le \Pi^{-2}\int_{\theta_1=0}^{\frac{(M-1)\Pi}{M}}\left\{1+P_1C(\theta_1)\delta_{SD}^2\right\}^{-1}d\theta_1$$
$$\int_{\theta_2=0}^{\frac{(M-1)\Pi}{M}}\begin{bmatrix}\left(M_{\beta_{\max}}\left(0.50\tilde{P}_2C(\theta_1)q_1^{-1}+0.50P_1C(\theta_2)q_2^{-1}\right)\right)\\ -M_{\beta_{\max}}\left(\left(P_1C(\theta_1)+\delta_{SD}^{-2}\right)\alpha+0.50\tilde{P}_2C(\theta_1)q_1^{-1}+0.50P_1C(\theta_2)q_2^{-1}\right)\end{bmatrix}d\theta_2. \tag{27}$$

Where $M_{\beta_{\max}}(\cdot)$ is the MGF of $\beta_{\max}$ and it can be approximated as [1, 20],

$$M_{\beta_{\max}}(\gamma) \approx L\sum_{n=0}^{L-1}\binom{L-1}{n}(-1)^nM_{\beta_m}(\gamma+0.50nt_2). \tag{28}$$

Where we applied $K_1(x) \approx x^{-1}$ and $M_{\beta_m}(\cdot)$ in the MGF of β_m. It is shown in [1, 20] that for two independent exponential RV with parameters λ_1 and λ_2, the MGF of their HMF is expressed in Eq. (29) [19, 20].

$$M_{\beta_m}(\gamma)=E_{\beta_m}(\exp(-\gamma\beta_m))=\frac{16\lambda_1\lambda_2}{3(\lambda_1+\lambda_2+2\sqrt{\lambda_1\lambda_2}+\gamma)^2}\times(\frac{4(\lambda_1+\lambda_2)\,{}_2F_1\left(3,\frac{3}{2};\frac{5}{2};\frac{\lambda_1+\lambda_2-\sqrt{\lambda_1\lambda_2}+\gamma}{\lambda_1+\lambda_2+\sqrt{\lambda_1\lambda_2}+\gamma}\right)}{(\lambda_1+\lambda_2+2\sqrt{\lambda_1\lambda_2}+\gamma)}$$
$$+\,{}_2F_1\left(2,\frac{1}{2};\frac{5}{2};\frac{\lambda_1+\lambda_2-\sqrt{\lambda_1\lambda_2}+\gamma}{\lambda_1+\lambda_2+\sqrt{\lambda_1\lambda_2}+\gamma}\right)). \tag{29}$$

Where $E_{\beta_m}(\cdot)$ represents the average value w.r.t. β_m and ${}_2F_1(.,.;.;.)$ is the Gauss hypergeometric function [1, 2, 14, 20]. Applying similar procedure as done in Eqs. (22)-(27), we get [1, 2, 5, 20],

$$P_r(B/\Phi^c)P_r(\Phi^c)\le\frac{1}{\Pi}\int_{\theta=0}^{\frac{(M-1)\Pi}{M}}(\frac{M_{\beta_{\max}}\left(0.50\tilde{P}_2C(\theta)q_1^{-1}\right)}{1+P_1C(\theta)\delta_{SD}^2}-\frac{M_{\beta_{\max}}\left(\left(PC(\theta)+\delta_{SD}^{-2}\right)\alpha+0.50\tilde{P}_2C(\theta)q_1^{-1}\right)}{1+P_1C(\theta)P_1C(\theta_2)})d\theta. \tag{30}$$

The unconditional error probability of the SRD mode can be expressed as [19, 20],

$$P_r(e/\Phi^c)P_r(\Phi^c) = P_r(A/\Phi^c)P_r(\Phi^c)\Big|_{\tilde{P}_2=0} - P_r(A/\Phi^c)P_r(\Phi^c)\Big|_{\tilde{P}_2=P_2} + P_r(B/\Phi^c)P_r(\Phi^c)\Big|_{\tilde{P}_2=P_2}, \quad (31)$$

$$P_r(e) \le L!\left(\frac{t_2\delta_{SD}^2}{2\alpha}\right)^L F_1\left(\prod_{n=0}^{L}\left(1+\frac{t_2\delta_{SD}^2 n}{2\alpha}+\frac{bP\delta_{SD}^2 A_1}{\eta_{SD}\sin^2(\theta)}\right)^2\right)+\sum_{n=0}^{L-1}\binom{L-1}{n}\frac{(-1)^n}{\Pi}\times$$
$$\int_{\theta_1}^{\frac{(M-1)\Pi}{M}}\left(\frac{M_{\beta_m}\left(\frac{bP_2A_1}{\eta_{SD}\sin^2(\theta_1)2q_1}+\frac{nt_2}{2}\right)}{\left(1+\frac{bP_1\delta_{SD}^2A_1}{\eta_{SD}\sin^2(\theta_1)}\right)^2}+\frac{\frac{1}{\Pi}\int_{\theta_2=0}^{\frac{(M-1)\Pi}{M}} M_{\beta_m}\left(\frac{bP_1A_1}{2q_2\eta_{SD}\sin^2(\theta_2)}+\frac{nt_2}{2}\right)d\theta_2}{\left(1+\frac{bP_1\delta_{SD}^2}{\eta_{SD}\sin^2\theta_1}\right)^2}\right)d\theta_1. \quad (32)$$

Since $P_r(A/\Phi^c)P_r(\Phi^c)|_{\tilde{P}_2=\tilde{P}_2}$ in Eq. (26) is a nonnegative term, therefore an upper bound on the PEP of SRD transmission mode can be derived by neglecting this term from Eq. (31). Moreover, we can neglect the negative term in Eqs. (27) and (30). Therefore, an upper bound on the total PEP can be derived by adding Eqs. (19), (27), and (30), after neglecting the negative terms, as given in Eq. (32). In Eq. (32), we apply identity $\sum_{n=0}^{L}\binom{L}{n}(-1)^n(x+ny)^{-1} = L!\,y^L\left\{\prod_{n=0}^{L}(x+ny)\right\}^{-1}$ [20] for direct SD PEP in Eq. (19).

3.2 DO Analysis

For getting the DO expression, we apply a high SNR approximation in Eq. (32), the approximated $P_r(e)$ is given as,

$$P_r(e) \le L!\left(\frac{t_2\delta_{SD}^2}{2\alpha}\right)^L F_1\left(\left(\frac{bP\delta_{SD}^2 A_1}{\eta_{SD}\sin^2(\theta)}\right)^{2(L+1)}\right)+\sum_{n=0}^{L-1}\binom{L-1}{n}\frac{(-1)^n}{\Pi}\int_{\theta_1}^{\frac{(M-1)\Pi}{M}}\frac{\eta_{SD}\sin^2\theta_1}{bP_1\delta_{SD}^2 A_1}$$
$$\times\left[M_{\beta_m}\left(\frac{bP_2}{2q_1\eta_{SD}\sin^2\theta_1}+\frac{nt_2}{2}\right)+\frac{1}{\Pi}\int_{\theta_2=0}^{\frac{(M-1)\Pi}{M}} M_{\beta_m}\left(\frac{bP_1}{2q_2\eta_{SD}\sin^2\theta_2}+\frac{nt_2}{2}\right)d\theta_2\right]d\theta_1. \quad (33)$$

Applying approximation of the MGF of two independent exponential RV $M_{\beta_{\max}}(\gamma) \approx 0.50(q_1\delta_{RD}^2 + q_2\delta_{SR}^2)\gamma^1$ [1, 2, 19, 20], we get,

$$P_r(e) \le L!\left(\frac{\eta_{SD}}{bP}\right)^{L+1}\left(\frac{t_2}{2\alpha}\right)^L\frac{I(2L+2)}{\delta_{SD}^2}+L!\,t_2^{L-1}\left(q_1\delta_{RD}^2+q_1\delta_{SR}^2\right)\times\frac{1}{\Pi}\int_{\theta_1=0}^{\frac{(M-1)\Pi}{M}}\frac{\eta_{SD}\sin^2\theta_1}{bP_1\delta_{SD}^2}$$
$$\times\left(\frac{1}{\prod_{n=0}^{L-1}\left(\frac{bP_2}{q_1\eta_{RD}\sin^2\theta_1}+nt_2\right)}+\frac{1}{\Pi}\int_{\theta_2=0}^{\frac{(M-1)\Pi}{M}}\frac{1}{\prod_{n=0}^{L-1}\left(\frac{bP_1}{q_2\eta_{SD}\sin^2\theta_2}+nt_2\right)}d\theta_2\right)d\theta_1. \quad (34)$$

$$P_r(e) \le L!\left(\frac{\eta_{SD}}{bP}\right)^{L+1}\left(\frac{t_2}{\alpha}\right)^{L}\frac{I(2L)}{\delta_{SD}^2} + L!\left(\frac{\eta_{RD}}{b}\right)^{L+1} t_2^{L-1}\frac{\left(q_1\delta_{RD}^2 + q_1\delta_{SR}^2\right)}{P_1\delta_{SD}^2} \times \left(\left(\frac{q_1}{P_2}\right)^{L} I(2L+2) + \left(\frac{q_2}{P_1}\right)^{L} AI(L)\right). \quad (35)$$

Where $I(p) = \frac{1}{\Pi}\int_{\theta=0}^{\frac{(M-1)\Pi}{M}} \sin^p(\theta)d\theta$. Substituting $q_1 = \frac{A^2}{g^2}, q_2 = \frac{B}{g(1-g)}$ and $t_2 = \frac{1}{q_2\delta_{SR}^2} + \frac{1}{q_1\delta_{RD}^2}$ and using $P_1 = gP$ and $P_2 = (1 - g)P$, we get,

$$P_r(e) \le \left[CG \times \frac{P}{\eta_{SD}}\right]^{-2(L+1)}. \quad (36)$$

Where CG denotes the coding gain expressed in Eq. (37).

$$CG = \left(\frac{L!\left(\frac{g(1-g)}{B\delta_{SR}^2} + \frac{g^2}{A^2\delta_{RD}^2}\right)^{2(L-1)}}{b^{2(L+1)}\delta_{SD}^2}\right) \times \left(\frac{\left(\frac{g(1-g)}{B\delta_{SR}^2} + \frac{g^2}{A^2\delta_{SR}^2}\right)I(2L)}{(2\alpha)^L} + \frac{\left(\frac{A^2\delta_{RD}^2}{g^2} + \frac{B\delta_{SR}^2}{g(1-g)}\right)\left(A^{2L}I(2L+2) + B^L I(L)\right)}{g^{L+1}(1-g)^L}\right)^{\frac{-1}{(L+1)}}. \quad (37)$$

The DO expression is given as, $DO = -Lim_{SNR\to\infty}\log(P_r(e)/\log(SNR))$. By substituting Eq. (35) in DO expression given above, we get, $DO = NN_D + NLmin(N, N_D)$.

3.3 Optimal Power Allocation

In the absence of cooperation, all the available power is transmitted through the SD fading link. In the cooperation mode, we find the optimal powers P_1 and P_2 which increase the end-to-end reliability subject to the power constraint $P_1 + P_2 \le P$. Substituting $q_1 = \frac{A^2}{g^2}$ and $q_2 = \frac{B}{g(1-g)}$ in Eq. (35) and using the relation $g = P_1/P$, we get,

$$\min_{P_1, P_2}\left\{\frac{\left(A^{2L+2}I(2L) + B^3A^L I(2L)\right)\delta_{RD}^2}{P_2^{2L+3}P_1^L} + \frac{\left(B^{2L}AI(4L) + AB^{L+1}I(2L+2)\right)\delta_{SR}^2}{P_1^{2L+2}P_2^{L+1}}\right\} s.t.\ P_1 + P_2 \le P. \quad (38)$$

The expression (38) is a basically a convex optimization [16-19] problem and it can be solved by using convex solver such as CVX software [15, 20].

4. SINGLE RELAY S-DF COOPERATION SCENARIO

4.1 PEP Analysis

In case of single relay based S-DF protocol, we consider path selection, *i.e.*, source selects either direct SD transmission path or relay assisted SRD transmission path. Let $\gamma_{\min}(p)$ be defined as [10], $\gamma_{\min}(p) = \min\{\gamma_{SR}(p), \gamma_{RD}(p)\}$. The Schematic representation of path selection based single relay S-DF cooperative communication protocol in given in Fig. 1 (b).

This metric is similar to the one given in [10, 14] for BRS over time varying fading channel. Let α is the cooperation threshold such that direct SD transmission mode is chosen for the event $\phi = \{\gamma_{SD}(p) \geq \alpha\gamma_{\min}(p)\}$ and relay assisted SRD transmission mode is chosen for $\bar{\phi} = \{\gamma_{SD}(p) < \alpha\gamma_{\min}(p)\}$ [10]. Let average PEP for the events $\bar{\phi}$ and ϕ respectively be defined as $P_r(e\cap\bar{\phi})$ and $P_r(e\cap\phi)$. The average PEP expression is modeled as [10, 18, 20],

$$\bar{P}_e = \underbrace{P_r(e\cap\phi)}_{DIRECT\ SD\ TRANSMISSION\ MODE} + \underbrace{P_r(e\cap\bar{\phi})}_{SRD\ TRANSMISSION\ MODE}. \tag{39}$$

$P_r(e\cap\phi)$ is modeled as [10, 18, 20],

$$P_r(e\cap\phi) = \int_0^\infty P_r(e/\phi, \gamma_{SD}(p))P_r(\phi/\gamma_{SD}(p))f_{\gamma_{SD}}(\gamma_{SD}(p))d\gamma_{SD}(p). \tag{40}$$

Where $P_r(\phi/\gamma_{SD}(p)) = F_{\gamma_{\min}}(\gamma_{SD}(p)/\alpha)$ and $F_{\gamma_{\min}}(x)$ presents the CDF of the SNR metric $\gamma_{\min}(p)$ and is modeled as [10, 18], $F_{\gamma_{\min}}(x) = F_{\gamma_{SR}}(x) + F_{\gamma_{RD}}(x) - F_{\gamma_{SR}}(x)F_{\gamma_{RD}}(x)$. For the event ϕ, $P_r(e/\phi, \gamma_{SD}(p))$ is given as [10, 18],

$$P_r(e|\phi, \gamma_{SD}(p)) = \frac{1}{\Pi}\int_0^{\frac{(M-1)\Pi}{M}} \exp(-\sin^2(\Pi/M)\gamma_{SD}(p)/\sin^2(\theta))d\theta. \tag{41}$$

Substituting the expressions of $P_r(e/\phi, \gamma_{SD}(p))$ and $P_r(\phi/\gamma_{SD}(p))$ given above in Eq. (40), $P_r(e\cap\phi)$ can be written as [10, 14, 18, 20],

$$\begin{aligned} P_r(e\cap\phi) &= \frac{1}{\Pi}\int_0^{(M-1)\Pi/M}\left[\int_0^\infty \exp\{-(\sin^2(\Pi/M)\gamma_{SD}(p)\}F_{\gamma_{SR}}(\frac{\gamma_{SD}(p)}{\alpha})f_{\gamma_{SD}}(\gamma_{SD}(p))d\gamma_{SD}(p)\right]d\theta \\ &+\frac{1}{\Pi}\int_0^{(M-1)\Pi/M}\left[\int_0^\infty \exp\{-(\sin^2(\Pi/M)\gamma_{SD}(p)\}F_{\gamma_{RD}}(\frac{\gamma_{SD}(p)}{\alpha})f_{\gamma_{SD}}(\gamma_{SD}(p))d\gamma_{SD}(p)\right]d\theta \\ &-\frac{1}{\Pi}\int_0^{(M-1)\Pi/M}\left[\int_0^\infty \exp\{-(\sin^2(\Pi/M)\gamma_{SD}(p)\}F_{\gamma_{SR}}(\frac{\gamma_{SD}(p)}{\alpha})F_{\gamma_{RD}}(\frac{\gamma_{SD}(p)}{\alpha})f_{\gamma_{SD}}(\gamma_{SD}(p))d\gamma_{SD}(p)\right]d\theta. \end{aligned} \tag{42}$$

Following Eq. (9), expressions for $F_{\gamma_{SR}}(\gamma_{SD}(p)\alpha^{-1})$, $F_{\gamma_{RD}}(\gamma_{SD}(p)\alpha^{-1})$ and $f_{\gamma_{SD}}(\gamma_{SD}(p))$ are modeled as [10, 18],

$$F_{\gamma_{SR}}\{\gamma_{SD}(p)/\alpha\} = \frac{\gamma\left(N^2, \alpha C_{SR}(p)\tilde{\delta}_{SR}^2/\gamma_{SD}(p)\right)}{(N^2-1)!},\ F_{\gamma_{RD}}\left(\gamma_{SD}(p)/\alpha\right) = \frac{\gamma\left(NN_D, \alpha C_{RD}(p)\tilde{\delta}_{RD}^2/\gamma_{SD}(p)\right)}{(NN_D-1)!}$$

and

$$f_{SD}(\gamma_{SD}(p)) = (\gamma_{SD}(p))^{NN_D-1}\left(C_{SD}(p)\tilde{\delta}_{SD}^2\right)^{-NN_D}\{(NN_D-1)!\}^{-1}\exp(-\gamma_{SD}(p)/C_{SD}(p)\tilde{\delta}_{SD}^2)$$

respectively. Substituting the expression of $F_{\gamma_{SR}}(\gamma_{SD}(p)/\alpha)$, $F_{\gamma_{SR}}(\gamma_{SD}(p)/\alpha)$ and $f_{SD}(\gamma_{SD}(p))$ into Eq. (42) and neglecting the negative term in Eq. (42), PEP upper bound in modeled as,

$$P_r(e\cap\phi) \leq \frac{1}{\Pi(N^2-1)!(NN_D-1)!(C_{SD}(p)\tilde{\delta}_{SD}^2)^{NN_D}}$$

$$\underbrace{\times\int_0^{(M-1)pi/M}\left[\int_0^{\infty}\exp\left\{-\left(\frac{\sin^2(pi/M)}{\sin^2(\theta)}+\frac{1}{C_{SD}(p)\tilde{\delta}_{SD}^2}\right)\gamma_{SD}(p)\right\}\times\gamma\left(N^2,\frac{1}{\alpha C_{SR}(p)\tilde{\delta}_{SR}^2}\right)\left(\gamma_{SD}(p)\right)^{NN_D-1}d\gamma_{SD}(p)\right]d\theta}_{P_r^1(e\cap\phi)}$$

$$+\underbrace{\frac{1}{\Pi(N^2-1)!(NN_D-1)!(C_{SD}(p)\tilde{\delta}_{SD}^2)^{NN_D}}\times\int_0^{(M-1)pi/M}\left[\int_0^{\infty}\exp\left\{-\left(\frac{\sin^2(pi/M)}{\sin^2(\theta)}+\frac{1}{C_{SD}(p)\tilde{\delta}_{SD}^2}\right)\gamma_{SD}(p)\right\}\times\gamma\left(N^2,\frac{1}{\alpha C_{SR}(p)\tilde{\delta}_{SR}^2}\right)\left(\gamma_{SD}(p)\right)^{NN_D-1}d\gamma_{SD}(p)\right]d\theta}_{P_r^2(e\cap\phi)} \tag{43}$$

Employing the identity $\int_0^x x^{\mu_1-1}e^{-\beta_1 x}\gamma(a_{11},\alpha_1 x)dx=\frac{\alpha_1^{a_{11}}(\mu_1+a_{11}-1)!}{a_{11}(\alpha_1+\beta_1)^{\mu_1+a_{11}}}\times {}_2F_1(1,\mu_1+a_{11};\ 1+a_{11};\ \frac{\alpha_1}{\alpha_1+\beta_1})$ [1, 20], $P_r^1(e\cap\phi)$ can be simplified as,

$$P_r^1(e\cap\phi)=\frac{(NN_D+N^2-1)!}{\Pi N^2!(NN_D-1)!(C_{SD}(p)\tilde{\delta}_{SD}^2)^{NN_D}(\alpha C_{SR}(p)\tilde{\delta}_{SR}^2)^{N^2}}\times$$
$$\int_0^{(M-1)pi/M}[(\frac{1}{(\frac{1}{\alpha C_{SR}(p)\tilde{\delta}_{SR}^2}+\frac{\sin^2(\frac{pi}{M})}{\sin^2(\theta)}+\frac{1}{C_{SD}(p)\tilde{\delta}_{SD}^2})^{NN_D+N^2}}\times {}_2F_1)(1,NN_D+N^2;N^2+1;\frac{1}{(\frac{1}{\alpha C_{SR}(p)\tilde{\delta}_{SR}^2}+\frac{\sin^2(\frac{pi}{M})}{\sin^2(\theta)}+\frac{1}{C_{SD}(p)\tilde{\delta}_{SD}^2})^{NN_D+N^2}})]d\theta.$$

Where ${}_2F_1(1,\mu_1+v_1;1+v_1;\frac{\alpha_1}{\alpha_1+\beta_1})$ denotes the ordinary hypergeometric function [10, 14]. Following the similar procedure $P_r^2(e\cap\phi)$ can be written as,

$$P_r^2(e\cap\phi)=\frac{(2NN_D-1)!}{\Pi NN_D!(NN_D-1)!(C_{SD}(p)\tilde{\delta}_{SD}^2)^{NN_D}(\alpha C_{RD}(p)\tilde{\delta}_{RD}^2)^{NN_D}}\times$$
$$\int_0^{(M-1)pi/M}\left[\frac{1}{\left(\frac{1}{\alpha C_{RD}(p)\tilde{\delta}_{RD}^2}+\frac{\sin^2(\frac{pi}{M})}{\sin^2(\theta)}+\frac{1}{C_{SD}(p)\tilde{\delta}_{SD}^2}\right)^{2NN_D}}\times {}_2F_1\left(1,2NN_D;NN_D+1;\frac{1}{\left(\frac{1}{\alpha C_{RD}(p)\tilde{\delta}_{RD}^2}+\frac{\sin^2(\frac{pi}{M})}{\sin^2(\theta)}+\frac{1}{C_{SD}(p)\tilde{\delta}_{SD}^2}\right)^{NN_D+N^2}}\right)\right]d\theta.$$

Substituting the expressions of $P_r^1(e\cap\phi)$ and $P_r^2(e\cap\phi)$ derived above and neglecting the negative term, *i.e.*, $P_r^3(e\cap\phi)$ yields the upper bound in (8) for error event $\phi=\{\gamma_{SD}(p)\}\geq\alpha\gamma_{\min}(p)$ corresponding to direct SD transmission, is expressed as,

$$P_r(e\cap\phi)\leq\frac{(NN_D+N^2-1)!}{\Pi N^2!(NN_D-1)!(C_{SD}(p)\tilde{\delta}_{SD}^2)^{NN_D}(\alpha C_{SR}(p)\tilde{\delta}_{SR}^2)^{N^2}}\times$$
$$\int_0^{(M-1)pi/M}\left[\frac{1}{\left(\frac{1}{\alpha C_{SR}(p)\tilde{\delta}_{SR}^2}+\frac{\sin^2(\frac{pi}{M})}{\sin^2(\theta)}+\frac{1}{C_{SD}(p)\tilde{\delta}_{SD}^2}\right)^{NN_D+N^2}}{}_2F_1\left(1,NN_D+N^2;N^2+1;\frac{1}{\left(\frac{1}{\alpha C_{SR}(p)\tilde{\delta}_{SR}^2}+\frac{\sin^2(\frac{pi}{M})}{\sin^2(\theta)}+\frac{1}{C_{SD}(p)\tilde{\delta}_{SD}^2}\right)^{NN_D+N^2}}\right)\right]d\theta$$

$$+\frac{(2NN_D-1)!}{\Pi NN_D!(NN_D-1)!(C_{SD}(p)\tilde{\delta}_{SD}^2)^{NN_D}(\alpha C_{RD}(p)\tilde{\delta}_{RD}^2)^{NN_D}}\times$$

$$\int_0^{(M-1)pi/M}\left[\frac{1}{\left(\frac{1}{\alpha C_{RD}(p)\tilde{\delta}_{RD}^2}+\frac{\sin^2(\frac{pi}{M})}{\sin^2(\theta)}+\frac{1}{C_{SD}(p)\tilde{\delta}_{SD}^2}\right)^{2NN_D}}\times {}_2F_1\left(1,2NN_D;NN_D+1;\frac{1}{\left(\frac{1}{\alpha C_{RD}(p)\tilde{\delta}_{RD}^2}+\frac{\sin^2(\frac{pi}{M})}{\sin^2(\theta)}+\frac{1}{C_{SD}(p)\tilde{\delta}_{SD}^2}\right)^{NN_D+N^2}}\right)\right]d\theta$$

(44)

The error probability corresponding to the event $\bar{\phi}=\{\gamma_{SD}(p)<\alpha\gamma_{\min}(p)\}$ can be derived analogously. The instantaneous SNR at the destination node for the SRD mode of transmission, *i.e.*, relay assisted transmission is well approximated as, $\gamma_{end\text{-}to\text{-}end}(p)=\min\{\gamma_{SR}(p),\gamma_{RD}(p)\}=\gamma_{\min}(p)$ [10, 14, 18]. The error probability expression for the event $\bar{\phi}=\{\gamma_{SD}(p)<\alpha\gamma_{\min}(p)\}$ is given as [10],

$$P_r(e\cap\bar{\phi})=\int_{\gamma_1}P_r\{e/\bar{\phi},\gamma_1)P_r\{\bar{\phi}/\gamma_1)f_{\gamma_1}(\gamma_1)d\gamma_1.$$

Where integration variable $\gamma_1\triangleq\{\gamma_{\min}(p),\gamma_{SD}(p)\}$.

Employing $P_r(e/\bar{\phi},\gamma_1)=\frac{1}{\Pi}\int_0^{\frac{(M-1)\Pi}{M}}\exp\left(-\frac{\sin^2(pi/M)\gamma_{\min}(p)}{\sin^2(\theta)}\right)d\theta$ leads to the following simplification [10, 18],

$$P_r(e\cap\bar{\phi})=\frac{1}{\Pi}\int_{\gamma_{\min}(p)=0}^{\infty}\int_{\theta=0}^{\frac{(M-1)\Pi}{M}}\exp\left(\frac{\sin^2(pi/M)}{\sin^2(\theta)}\right)\times\underbrace{\int_{\gamma_{SD}(p)=0}^{\alpha\gamma_{\min}(p)}f_{\gamma_{SD}}(\gamma_{SD}(p))d\gamma_{SD}(p)}_{F_{\gamma_{SD}}(\alpha\gamma_{\min}(p))}f_{\gamma_{\min}}(\gamma_{\min}(p))d\gamma_{\min}(p)$$

(45)

The term $f_{\gamma_{\min}}(x)$ represents the PDF of $\gamma_{\min}(p)$ and is expressed as [10, 18], $f_{\gamma_{\min}}(x)=f_{\gamma_{SR}}(x)+f_{\gamma_{RD}}(x)-F_{\gamma_{SR}}(x)f_{\gamma_{RD}}(x)-F_{\gamma_{RD}}(x)f_{\gamma_{SR}}(x)$. Employing $f_{\gamma_{\min}}(x)$ in Eq. (45), $P_r(e\cap\bar{\phi})$ is modeled as,

$$P_r(e\cap\bar{\phi})=\underbrace{\frac{1}{pi}\int_0^{\frac{(M-1)pi}{M}}\left[\int_0^{\infty}P_r(e/\bar{\phi},\gamma_{SD}(p)P_r(\bar{\phi}/\gamma_{SD}(p))\underbrace{\int_{\gamma_{SD}(p)=0}^{\alpha\gamma_{\min}(p)}f_{\gamma_{SD}}(\gamma_{SD}(p))d\gamma_{SD}(p)}_{F_{\gamma_{SD}}(\alpha\gamma_{\min}(p))}f_{\gamma_{SR}}(\gamma_{\min}(p))d\gamma_{\min}(p)\right]d\theta}_{P_r^1(e\cap\bar{\phi})}$$

$$+\underbrace{\frac{1}{pi}\int_0^{\frac{(M-1)pi}{M}}\left[\int_0^{\infty}P_r(e/\bar{\phi},\gamma_{SD}(p))P_r(\bar{\phi}/\gamma_{SD}(p))\underbrace{\int_{\gamma_{SD}(p)=0}^{\alpha\gamma_{\min}(p)}f_{\gamma_{SD}}(\gamma_{SD}(p))d\gamma_{SD}(p)}_{F_{\gamma_{SD}}(\alpha\gamma_{\min}(p))}f_{\gamma_{RD}}(\gamma_{\min}(p))d\gamma_{\min}(p)\right]d\theta}_{P_r^2(e\cap\bar{\phi})}$$

$$\underbrace{\frac{1}{pi}\int_{0}^{\frac{(M-1)pi}{M}}\left[\int_{0}^{\infty}P_r(e/\bar{\phi},\gamma_{SD}(p))P_r(\bar{\phi}/\gamma_{SD}(p))\underbrace{\int_{\gamma_{SD}(p)=0}^{\alpha\gamma_{\min}(p)} f_{\gamma_{SD}}(\gamma_{SD}(p))d\gamma_{SD}(p)}_{F_{\gamma_{SD}}(\alpha\gamma_{\min}(p))}F_{\gamma_{SR}}(\gamma_{\min}(p))f_{\gamma_{RD}}(\gamma_{\min}(p))d\gamma_{\min}(p)\right]d\theta}_{P_r^3(e\cap\bar{\phi})}$$

$$\underbrace{\frac{1}{pi}\int_{0}^{\frac{(M-1)pi}{M}}\left[\int_{0}^{\infty}P_r(e/\bar{\phi},\gamma_{SD}(p))P_r(\bar{\phi}/\gamma_{SD}(p))\underbrace{\int_{\gamma_{SD}(p)=0}^{\alpha\gamma_{\min}(p)} f_{\gamma_{SD}}(\gamma_{SD}(p))d\gamma_{SD}(p)}_{F_{\gamma_{SD}}(\alpha\gamma_{\min}(p))}F_{\gamma_{RD}}(\gamma_{\min}(p))f_{\gamma_{SR}}(\gamma_{\min}(p))d\gamma_{\min}(p)\right]d\theta}_{P_r^4(e\cap\bar{\phi})} \tag{46}$$

Following Eq. (9), $F_{\gamma_{SD}}(\alpha\gamma_{\min}(p))$ and $f_{\gamma_{SR}}(\gamma_{\min}(p))$ can be written as,

$$F_{\gamma_{SD}}(\alpha\gamma_{\min}(p))=\frac{\gamma\left(NN_D,\frac{\alpha}{C_{SD}(p)\tilde{\delta}_{SD}^2}\gamma_{\min}(p)\right)}{(NN_D-1)!}\text{ and } f_{\gamma_{SR}}(\gamma_{\min}(p))=\frac{(\gamma_{\min}(p))^{N^2-1}}{\left(C_{SR}(p)\tilde{\delta}_{SR}^2\right)^{N^2}(N^2-1)!}\exp\left(-\frac{\gamma_{\min}(p)}{C_{SR}(p)\tilde{\delta}_{SR}^2}\right)$$

respectively. Using expressions of $F_{\gamma_{SD}}(\alpha\gamma_{\min}(p))$ and $f_{\gamma_{SR}}(\gamma_{\min}(p))$ and employing the identity $\int_0^x x^{\mu_1-1}e^{-\beta_1 x}\gamma(\varsigma_1,\alpha_1 x)dx=\frac{\alpha_1^{\varsigma_1}(\mu_1+\varsigma_1-1)!}{\varsigma_1(\alpha_1+\beta_1)^{\mu_1+\varsigma_1}}\times {}_2F_1(1,\mu_1+\varsigma_1;1+\varsigma_1;\frac{\alpha_1}{\alpha_1+\beta_1})$ [1, 10, 14, 19], $P_r^1(e\cap\phi)$ can be simplified as,

$$P_r^1(e\cap\bar{\phi})=\frac{(N^2+NN_D-1)!}{\Pi(N^2-1)!NN_D!}\left(\frac{1}{C_{SR}(p)\tilde{\delta}_{SR}^2}\right)^{N^2}\left(\frac{\alpha}{C_{SD}(p)\tilde{\delta}_{SD}^2}\right)^{NN_D}\times$$
$$\int_0^{\frac{(M-1)\Pi}{M}}\left[\frac{1}{\left(\frac{\alpha}{C_{SD}(p)\tilde{\delta}_{SD}^2}+\frac{\sin^2(\frac{pi}{M})}{\sin^2(\theta)}+\frac{1}{C_{SR}(p)\tilde{\delta}_{SR}^2}\right)^{N^2+NN_D}}\times{}_2F_1\left(1,N^2+NN_D;NN_D+1;\frac{\frac{\alpha}{C_{SD}(p)\tilde{\delta}_{SD}^2}}{\frac{\alpha}{C_{SD}(p)\tilde{\delta}_{SD}^2}+\frac{\sin^2(\frac{pi}{M})}{\sin^2(\theta)}+\frac{1}{C_{SR}(p)\tilde{\delta}_{SR}^2}}\right)\right]d\theta \tag{47}$$

Following Eq. (9) $f_{\gamma_{RD}}(\gamma_{\min}(p))$ can be written as,

$$f_{\gamma_{RD}}(\gamma_{\min}(p))=\left(\frac{1}{C_{RD}(p)\tilde{\delta}_{RD}^2}\right)^{NN_D}\frac{(\gamma_{\min}(p))^{NN_D-1}}{(NN_D-1)!}\exp\left(-\frac{\gamma_{\min}(p)}{C_{RD}(p)\tilde{\delta}_{RD}^2}\right).$$

Using expressions of $f_{\gamma_{RD}}(\gamma_{\min}(p))$ and employing the identity

$\int_0^x x^{\mu_1-1}e^{-\beta_1 x}\gamma(v_1,\alpha_1 x)dx=\frac{\alpha_1^{v_1}(\mu_1+v_1-1)!}{v_1(\alpha_1+\beta_1)^{\mu_1+v_1}}\times{}_2F_1(1,\mu_1+v_1;1+v_1;\frac{\alpha_1}{\alpha_1+\beta_1})$ [1, 19], $P_r^2(e\cap\phi)$ can be simplified as,

$$P_r^2(e\cap\phi)=\frac{(2NN_D-1)!}{\Pi NN_D!(NN_D-1)!(C_{SD}(p)\tilde{\delta}_{SD}^2)^{NN_D}(\alpha C_{RD}(p)(\tilde{\delta}_{RD}^2)^{NN_D}}\times$$

$$\int_0^{(M-1)pi/M}\left[\frac{1}{\left(\frac{1}{\alpha C_{RD}(p)\tilde{\delta}_{RD}^2}+\frac{\sin^2(\frac{pi}{M})}{\sin^2(\theta)}+\frac{1}{C_{SD}(p)\tilde{\delta}_{SD}^2}\right)^{2NN_D}}F_1\left(1,2NN_D;NN_D+1;\frac{1}{\left(\frac{1}{\alpha C_{RD}(p)\tilde{\delta}_{RD}^2}+\frac{\sin^2(\frac{pi}{M})}{\sin^2(\theta)}+\frac{1}{C_{SD}(p)\tilde{\delta}_{SD}^2}\right)^{NN_D+N^2}}\right)\right]d\theta \tag{48}$$

Substituting the expressions of $P_r^1(e\cap\phi)$ and $P_r^2(e\cap\phi)$ derived in Eqs. (47) and (48) and neglecting the negative term, *i.e.*, $P_r^2(e\cap\bar{\phi})$ and $P_r^4(e\cap\bar{\phi})$ yields the upper bound in (46) for error event $\bar{\phi}=\{\gamma_{SD}<\alpha\gamma_{\min}\}$ corresponding to relay assisted SRD transmission, is expressed as,

$$P_r(e\cap\bar{\phi})\le\frac{(N^2+NN_D-1)!}{\Pi(N^2-1)!NN_D!}\left(\frac{1}{C_{SR}(p)\tilde{\delta}_{SR}^2}\right)^{N^2}\left(\frac{\alpha}{C_{SD}(p)\tilde{\delta}_{SD}^2}\right)^{NN_D}\times$$

$$\int_0^{\frac{(M-1)\Pi}{M}}\left[\frac{1}{\left(\frac{\alpha}{C_{SD}(p)\tilde{\delta}_{SD}^2}+\frac{\sin^2(\frac{pi}{M})}{\sin^2(\theta)}+\frac{1}{C_{SR}(p)\tilde{\delta}_{SR}^2}\right)^{N^2+NN_D}}{}_2F_1\left(1,N^2+NN_D;NN_D+1;\frac{\frac{\alpha}{C_{SD}(p)\tilde{\delta}_{SD}^2}}{\frac{\alpha}{C_{SD}(p)\tilde{\delta}_{SD}^2}+\frac{\sin^2(\frac{pi}{M})}{\sin^2(\theta)}+\frac{1}{C_{SR}(p)\tilde{\delta}_{SR}^2}}\right)\right]d\theta$$

$$+\frac{(2NN_D-1)!}{\Pi NN_D!(NN_D-1)!(C_{SD}(p)\tilde{\delta}_{SD}^2)^{NN_D}(\alpha C_{RD}(p)\tilde{\delta}_{RD}^2)^{NN_D}}\times$$

$$\int_0^{(M-1)pi/M}\left[\frac{1}{\left(\frac{1}{\alpha C_{RD}(p)\tilde{\delta}_{RD}^2}+\frac{\sin^2(\frac{pi}{M})}{\sin^2(\theta)}+\frac{1}{C_{SD}(p)\tilde{\delta}_{SD}^2}\right)^{2NN_D}}F_1\left(1,2NN_D;NN_D+1;\frac{1}{\left(\frac{1}{\alpha C_{RD}(p)\tilde{\delta}_{RD}^2}+\frac{\sin^2(\frac{pi}{M})}{\sin^2(\theta)}+\frac{1}{C_{SD}(p)\tilde{\delta}_{SD}^2}\right)^{NN_D+N^2}}\right)\right]d\theta \tag{49}$$

Substituting the expressions of $P_r(e\cap\phi)$ and $P_r(e\cap\bar{\phi})$ given in Eqs. (44) and (49) respectively in Eq. (39), yields the average PEP bound for path selection based S-DF as,

$$P_r\le\frac{(NN_D+N^2-1)!}{\Pi N^2!(NN_D-1)!(C_{SD}(p)\tilde{\delta}_{SD}^2)^{NN_D}(\alpha C_{SR}(p)\tilde{\delta}_{SR}^2)^{N^2}}\times$$

$$\int_0^{(M-1)pi/M}\left[\frac{1}{\left(\frac{1}{\alpha C_{SR}(p)\tilde{\delta}_{SR}^2}+\frac{\sin^2(\frac{pi}{M})}{\sin^2(\theta)}+\frac{1}{C_{SD}(p)\tilde{\delta}_{SD}^2}\right)^{NN_D+N^2}}{}_2F_1\left(1,NN_D+N^2;N^2+1;\frac{1}{\left(\frac{1}{\alpha C_{SR}(p)\tilde{\delta}_{SR}^2}+\frac{\sin^2(\frac{pi}{M})}{\sin^2(\theta)}+\frac{1}{C_{SD}(p)\tilde{\delta}_{SD}^2}\right)^{NN_D+N^2}}\right)\right]d\theta$$

$$+\frac{(2NN_D-1)!}{\Pi NN_D!(NN_D-1)!(C_{SD}(p)\tilde{\delta}_{SD}^2)^{NN_D}(\alpha C_{RD}(p)\tilde{\delta}_{RD}^2)^{NN_D}}\times$$

$$\int_0^{(M-1)pi/M}\left[\frac{1}{\left(\frac{1}{\alpha C_{RD}(p)\tilde{\delta}_{RD}^2}+\frac{\sin^2(\frac{pi}{M})}{\sin^2(\theta)}+\frac{1}{C_{SD}(p)\tilde{\delta}_{SD}^2}\right)^{2NN_D}}\,{}_2F_1\left(1,2NN_D;NN_D+1;\frac{1}{\left(\frac{1}{\alpha C_{RD}(p)\tilde{\delta}_{RD}^2}+\frac{\sin^2(\frac{pi}{M})}{\sin^2(\theta)}+\frac{1}{C_{SD}(p)\tilde{\delta}_{SD}^2}\right)^{NN_D+N^2}}\right)\right]d\theta$$

$$+\ \frac{(N^2+NN_D-1)!}{\Pi(N^2-1)!NN_D!}\left(\frac{1}{C_{SR}(p)\tilde{\delta}_{SR}^2}\right)^{N^2}\left(\frac{\alpha}{C_{SD}(p)\tilde{\delta}_{SD}^2}\right)^{NN_D}\times$$

$$\int_0^{\frac{(M-1)\Pi}{M}}\left[\frac{1}{\left(\frac{\alpha}{C_{SD}(p)\tilde{\delta}_{SD}^2}+\frac{\sin^2(\frac{pi}{M})}{\sin^2(\theta)}+\frac{1}{C_{SR}(p)\tilde{\delta}_{SR}^2}\right)^{N^2+NN_D}}\,{}_2F_1\left(1,N^2+NN_D;NN_D+1;\frac{\frac{\alpha}{C_{SD}(p)\tilde{\delta}_{SD}^2}}{\frac{\alpha}{C_{SD}(p)\tilde{\delta}_{SD}^2}+\frac{\sin^2(\frac{pi}{M})}{\sin^2(\theta)}+\frac{1}{C_{SR}(p)\tilde{\delta}_{SR}^2}}\right)\right]d\theta$$

$$+\ \frac{(2NN_D-1)!}{\Pi NN_D!(NN_D-1)!(C_{SD}(p)\tilde{\delta}_{SD}^2)^{NN_D}(\alpha C_{RD}(p)\tilde{\delta}_{RD}^2)^{NN_D}}\times$$

$$\int_0^{(M-1)pi/M}\left[\frac{1}{\left(\frac{1}{\alpha C_{RD}(p)\tilde{\delta}_{RD}^2}+\frac{\sin^2(\frac{pi}{M})}{\sin^2(\theta)}+\frac{1}{C_{SD}(p)\tilde{\delta}_{SD}^2}\right)^{2NN_D}}\,{}_2F_1\left(1,2NN_D;NN_D+1;\frac{1}{\left(\frac{1}{\alpha C_{RD}(p)\tilde{\delta}_{RD}^2}+\frac{\sin^2(\frac{pi}{M})}{\sin^2(\theta)}+\frac{1}{C_{SD}(p)\tilde{\delta}_{SD}^2}\right)^{NN_D+N^2}}\right)\right]d\theta \tag{50}$$

4.2 DO and Optimal Power Allocation Analysis

We demonstrate the optimal source-relay power allocation for path selection based S-DF cooperative communication protocol. For analysis purposes, at high SNR conditions, we consider that all nodes are static and perfect CSI conditions, *i.e.*, $\upsilon_{SD}=\upsilon_{SR}=\upsilon_{RD}=1$, $\sigma_{\in_{SD}}=\sigma_{\in_{SR}}=\sigma_{\in_{RD}}=0$ and $\sigma_{e_{SD}}=\sigma_{e_{SD}}=\sigma_{e_{SD}}=0$. Using the identity ${}_2F_1(a_1, b_1; c_1; z_1)=\sum_{n=0}^{\infty}\frac{(a_1)_{(n)}(b_1)_{(n)}(z_1)^n}{(c_1)_{(n)}n!}$ [10, 14, 19] and taking the dominant terms corresponding to $n=0$, simplified expression of the average PEP upper bound can be expressed as,

$$\begin{aligned}P_r \le\ & \frac{(NN_D+N^2-1)!(NR_C)^{NN_D+2N^2N^2}\xi(NN_D+N^2)(P/P_0)^{N^2}}{\Pi N^2!(NN_D-1)!(\delta_{SD}^2)^{NN_D}(\alpha\delta_{SR}^2)^{N^2}(\sin^2(pi/M))^{NN_D+N^2}}(N_0/P)^{NN_D+N^2}\\
&+\frac{(2NN_D-1)!(NR_C)^{2NN_D}\xi(2NN_D)(P/P_1)^{NN_D}}{\Pi NN_D!(NN_D-1)!(\delta_{SD}^2)^{NN_D}(\alpha\delta_{RD}^2)^{NN_D}(\sin^2(pi/M))^{2NN_D}}(N_0/P)^{2NN_D}\\
&+\frac{(N^2+NN_D-1)!(NR_C)^{NN_D+N^2}\alpha^{NN_D}\xi(NN_D+N^2)\left(P/P_0\right)^{N^2}}{\Pi(N^2-1)!(NN_D)!(\delta_{SR}^2)^{N^2}(\delta_{SD}^2)^{NN_D}(\sin^2(pi/M))^{NN_D+N^2}}\left(N_0/P\right)^{NN_D+N^2}\\
&+\frac{(2NN_D-1)!(NR_C)^{2NN_D}\alpha^{NN_D}\xi(2NN_D)}{\Pi(NN_D)((NN_D-1)!)^2(\delta_{SD}^2)^{NN_D}(\sin^2(pi/M))^{2NN_D}}\left(P/P_1\right)^{NN_D}\left(N_0/P\right)^{2NN_D}\end{aligned}\tag{51}$$

The average PEP upper bound derived in Eq. (16) can be further simplified as,

$$P_r \leq K_1(N_0/P)^{NN_D+N^2} + K_2(N_0/P)^{2NN_D} + K_3(N_0/P)^{NN_D+N^2} + K_4(N_0/P)^{2NN_D}. \tag{52}$$

Where K_1, K_2, K_3 and K_4 are suitably defined constant terms. DO can be derived as,

$$DO = -\lim_{\frac{P}{N_0}\to\infty} \frac{\log(P_r)}{\log(P/N_0)} = \min(NN_D,\ NN)\,. \tag{53}$$

Let the optimal source-relay power allocation factors a_0 and a_1 for the SRD transmission be P_0/P and P_1/P respectively. Substituting a_0 and a_1 in Eq. (51), average PEP upper bound can be further simplified as,

$$P_r \leq \frac{C_1}{(a_0)^{N^2}} + \frac{C_2}{(a_1)^{NN_D}}. \tag{54}$$

Where C_1 and C_2 are appropriately defined constant terms, given below,

$$C_1 = (N_0/P)^{NN_D+N^2}\left[\begin{array}{l}\dfrac{(NN_D+N^2-1)!(NR_C)^{NN_D+2N^2N^2}\,\xi(NN_D+N^2)}{\Pi N^2!(NN_D-1)!(\delta_{SD}^2)^{NN_D}(\alpha\delta_{SR}^2)^{N^2}(\sin^2(pi/M))^{NN_D+N^2}}\\ +\dfrac{(N^2+NN_D-1)!(NR_C)^{NN_D+N^2}\,\alpha^{NN_D}\,\xi(NN_D+N^2)}{\Pi(N^2-1)!(NN_D)!(\delta_{SR}^2)^{N^2}(\delta_{SD}^2)^{NN_D}(\sin^2(pi/M))^{NN_D+N^2}}\end{array}\right],$$

$$C_2 = (N_0/P)^{2NN_D}\left[\begin{array}{l}\dfrac{(2NN_D-1)!(NR_C)^{2NN_D}\,\xi(2NN_D)}{\Pi NN_D!(NN_D-1)!(\delta_{SD}^2)^{NN_D}(\alpha\delta_{RD}^2)^{NN_D}(\sin^2(pi/M))^{2NN_D}}\\ +\dfrac{(2NN_D-1)!(NR_C)^{2NN_D}\,\alpha^{NN_D}\,\xi(2NN_D)}{\Pi(NN_D)((NN_D-1)!)^2(\delta_{SD}^2)^{NN_D}(\sin^2(pi/M))^{2NN_D}}\end{array}\right].$$

Further, average PEP upper bound expression given in Eq. (54) can be modeled as a convex optimization (CO) problem of deriving the optimal source-relay power allocation factor (OPF) a_0 and a_1, as expressed below:

$$\min_{a_0,\,a_1}\left\{\frac{C_1}{(a_0)^{N^2}} + \frac{C_2}{(a_1)^{NN_D}}\right\} s.t.\ \ a_0 + a_1 \leq 1. \tag{55}$$

The Karush Kuhn Tucker (KKT) based CO method can be used to evaluate the optimal source-relay power allocation factor a_0 and a_1. Differentiating Eq. (55) and setting the resultant expression to zero that the OPF a_0 is expressed as the non-negative value of the quadratic expression,

$$C_2N_D(a_0)^{N^2+1} - C_1N(1-a_1)^{NN_D+1} = 0. \tag{56}$$

Eq. (56) can be solved by using standard software such as MATLAB.

5. NODE MOBILITY IMPACT AND ASYMPTOTIC FLOOR

Further, to represent the impact of mobile nodes and imperfect CSI on the system performance, one can evaluate the asymptotic error floor by ignoring N_0 in Eqs. (4) and (5) at high SNR *i.e.*, $\bar{\gamma}_{SR}(p)$, $\bar{\gamma}_{RD}(p) \to \infty$ and substituting the resulting expressions in Eqs. (32) and (50) [7] where the terms $\tilde{\eta}_{SD}$, $\tilde{\eta}_{SR}[i]$ and $\tilde{\eta}_{RD}[i]$ are defined as [14-16, 19],

$$\tilde{\eta}_{SD} = \upsilon_{SD}^{2(k-1)}\sigma_{\epsilon_{SD}}^2 + (1-\upsilon_{SD}^{2(k-1)})\sigma_{e_{SD}}^2, \tag{57}$$

$$\tilde{\eta}_{SR}[i] = (\upsilon_{SR}[i])^{2(k-1)}(\sigma_{\epsilon_{SR}}^{(i)})^2 + (1-(\upsilon_{SR}[i])^{2(k-1)})(\sigma_{e_{SR}}^{(i)})^2, \tag{58}$$

$$\tilde{\eta}_{RD}[i] = (\upsilon_{RD}[i])^{2(k-1)}(\sigma_{\epsilon_{RD}}^{(i)})^2 + (1-(\upsilon_{RD}[i])^{2(k-1)})(\sigma_{e_{RD}}^{(i)})^2. \tag{59}$$

Various cases arise due to mobility of SN, DN and RN, as expressed below:

Case 1: In this case we consider mobile SN and static RN and DN *i.e.*, $\upsilon_{SR}[i] < 1$, $\upsilon_{SD} < 1$, and $\upsilon_{RD}[i] = 1 \forall i$. Also we consider the perfect CSI scenario for MRC detection. In this scenario, it can be easily seen both the quantities $\tilde{\eta}_{SR}[i]$ and $\tilde{\eta}_{SD}$ are non-zero quantities and $\tilde{\eta}_{RD}[i] = 0$ because $\upsilon_{RD}[i] = 1 \forall i$. Also, we consider the perfect CSI scenario for MRC detection. Therefore, every PEP term relating to the states $[0, 0, 0, \ldots, 0, 1]^T$, $[0, 0, 0, \ldots, 1, 0]^T$, $[0, 0, 0, \ldots, 1, 1]^T$, …, $[1, 1, 1, \ldots, 1, 1]^T$ in Eqs. (32) and (50) equal to zero because $S_3^k[n] = 0$ for $1 \le n \le 2^L - 1$ [7, 10, 14, 20]. In this scenario, just the PEP terms relating to the states $[0, 0, 0, \ldots, 0, 0]^T$ contributes in Eqs. (32) and (50), which exhibit that the wireless framework encounters an asymptotic error floor because of the mobile SN.

Case 2: Let us consider RN and SN are static and only the DN is mobile *i.e.*, υ_{SD}, $\upsilon_{RD}[i] < 1$ and $\upsilon_{SR}[i] = 1 \forall i$. Also, we consider the perfect CSI scenario for MRC detection. Further $\tilde{\eta}_{SR}[i]$ zero because $\upsilon_{SR}[i] = 1$ and under this scenario, it can be easily seen that the quantities $\tilde{\eta}_{SD}$ and $\tilde{\eta}_{RD}[i]$ are non-zero $\forall i$.

Therefore, every PEP term relating to the state $[0, 0, 0, \ldots, 0, 0]^T$, $[0, 0, 0, \ldots, 0, 1]^T$, $[0, 0, 0, \ldots, 1, 0]^T$, …, $[1, 1, 1, \ldots, 1, 0]^T$ in Eqs. (32) and (50) tends to zero because $S_1^k(n) = 0$ for $0 \le n \le 2^L - 2$. In this scenario, just the PEP expression relating to the state $[1, 1, 1, \ldots, 1, 0]^T$ contributes in Eqs. (32) and (50), which exhibit that the wireless framework encounters an error-floor because of the mobility of DN [7, 10, 14, 20].

Case 3: Let us consider DN and SN are static and RN is mobile *i.e.*, $\upsilon_{SR}[i]$, $\upsilon_{RD}[i] < 1 \forall i$ and $\upsilon_{SD} = 1$. Also, we consider the perfect CSI scenario for MRC detection. In this case $\tilde{\eta}_{SD}$ is zero because $\upsilon_{SD} = 1$ and under this scenario, it can be easily observed that the terms $\tilde{\eta}_{SR}[i]$ and $\tilde{\eta}_{RD}[i]$ are non-zero. Therefore, in this scenario asymptotic error floor reduces to zero because all the PEP term relating to the states $[0, 0, 0, \ldots, 0, 0]^T$, $[0, 0, 0, \ldots, 0, 1]^T$, $[0, 0, 0, \ldots, 1, 0]^T$, …, $[1, 1, 1, \ldots, 1, 1]^T$, …, $[1, 1, 1, \ldots, 1, 1]^T$ in Eqs. (32) and (50) tends to zero. This case arises because of the fact that the terms $S_3^k(n) = 0$; $1 \le n \le 2^L - 1$ are reduced to zero for $\tilde{\eta}_{SD} = 0$ [7, 10, 14, 20].

Table 1. Obtained DO for BRS and Conventional S-DF protocol in various conditions.

Node Mobility scenario	DO
SN, RN and DN are mobile (Direct SD transmission)	0
SN, RN and DN are static (Path Selection Based single relay S-DF cooperation protocol)	$\min(NN_D, NN)$
SN, RN and DN are static (BRS based S-DF Protocol)	$NN_D+NL\min(N, N_D)$
SN and DN are static, RN are mobile (Conventional S-DF)	NN_D
SN, RN and DN are static, DO of RD link = DO of SR link (Conventional S-DF Protocol) [15]	$LNN+NN_D$
SN, RN and DN are static, DO of RD link > DO of SR link (Conventional S-DF Protocol) [15]	$KNN+NN_D$
SN, RN and DN are static, DO of RD link < DO of SR link (Conventional S-DF Protocol) [15]	KNN_D+NN_D
SN, RN and DN are static (Conventional S-DF Protocol) [15]	$NN_D+NL\min(N, N_D)$

6. SIMULATION RESULTS AND DISCUSSIONS

Monte Carlo simulations have been carried out in this section for verification of analytical results for S-DF cooperation protocol derived in the previous sections. In simulations, Alamouti STBC code is used; code-word symbols are 4-PSK modulated. Simulation parameters are given as, $f_c = 5.90\times10^9$ GHz, $R_S = 9600$ bps, $N_0 = 1$, $R_C = 1$, $\sigma^2_{\epsilon_i} = \{0.01\}$; $i \in \{SD, SR, RD\}$, $N = 2$, $N_D = 2$, $\sigma^2_{e_i} = \{0.01\}$; $i\in\{SD, SR, RD\}$. For perfect CSI, we take $\sigma^2_{\epsilon_i} = 0$. Figs. 2-8 demonstrate the end-to-end error probability performance of multi-hop BRS based S-DF and conventional multiple hop cooperative communication protocol. Simulation results exactly match with analytical results at high SNR regimes. Also, simulation outcomes confirm that in the case of static nodes and perfect CSI, conventional multiple hop S-DF cooperation protocol protocols achieves full DO which is equal to $NN_D+NL\min\{N, N_D\} = 12$. In Table 1 we have given various DO expressions for various node mobility conditions. Figs. 2-4 show that per-block average PEP performance degrades due to the presence of mobility and imperfect channel estimation. In the presence of these practical constraints the PEP performance is lower in comparison to PEP performance when all nodes are static and knowledge of perfect CSI, that is, $\nu_i = 1$; $i \in \{SD, SR, RD\}$. The simulation outcomes show that with an increase in cellular user's velocity v_p the PEP performance decreases because of the increase in value of the channel correlation coefficient ν_i. Results verify that, in case of node mobility S-DF protocol experiences error floors. Fig. 3 shows plots between per-block average PEP versus SNR in dB at optimal power factors β_0, β_f, $1 \leq f \leq 2$ obtained by solving the CO problem given previous sections by using CO solver such as CVX solver software for S-DF protocols with $L = 2$ relay nodes. From Fig. 4, it can be seen that system performance improves by using optimal power allocation factors in comparison when $\beta_0 = 1/3$, $\beta_1 = 1/3$, $\beta_2 = 1/3$ for several channel scenarios. Also system performance for optimal power allocation is more promising when the RD link variance is very high as compared to the SR link variance. This system performance improves because of the fact that when the RD link variance is very high as compared to the SR link variance, almost all available power is allocated to SN for better reception at the RN because SR link strength is very low. In other word the probability of error free decoding at the relay node and destination node is

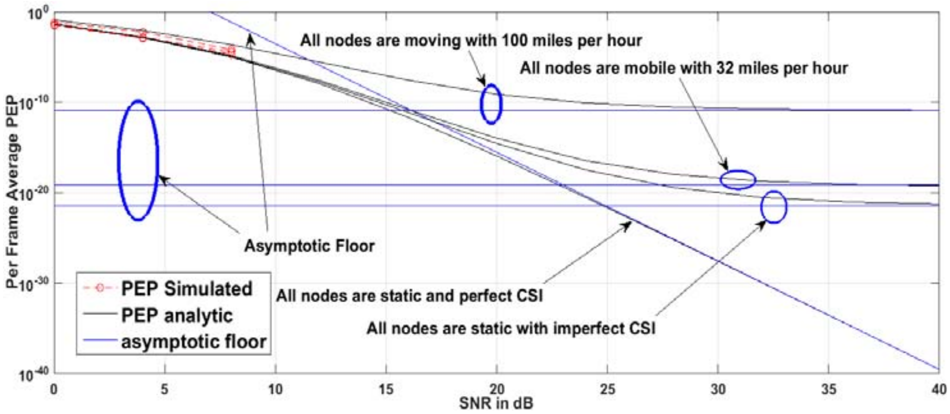

Fig. 2. Per block average PEP versus SNR in dB for BRS based S-DF protocol with $\delta_{SD}^2 = \delta_{SR}^2 = 10$, $\delta_{RD}^2 = 1$, $\nu = \{0.9915, 0.9189\}$, $v_P \in \{32, 100\}$mph, $\sigma_{\epsilon_i} = 0.01$, $\sigma_{e_i} = 0.10$, $M_b = 15$ and $L = 2$.

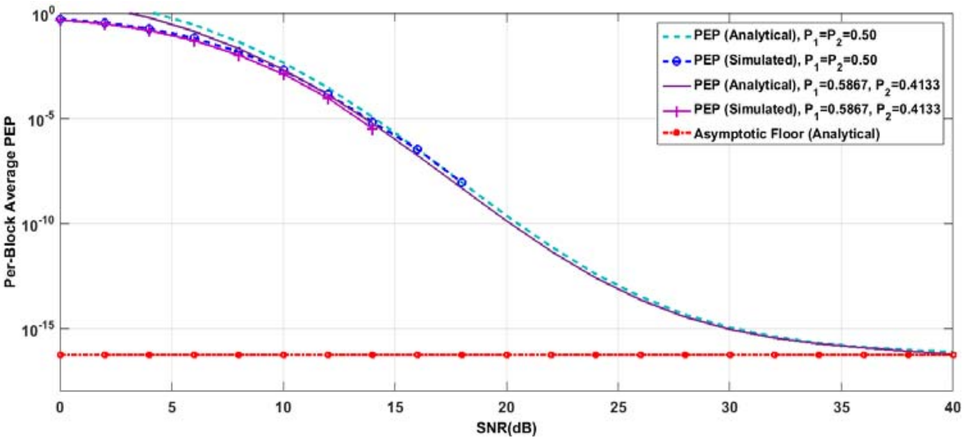

Fig. 3. Per-block average PEP versus SNR in dB for BRS based S-DF protocol for optimal power allocation, simulation parameters are $\delta_{SD}^2 = 1$, $\delta_{SR}^2 = 10$, $\delta_{RD}^2 = 50$, $\sigma_{e_i} = 0.10$, $L = 2$, $\nu = 0.9724$, $N_0 = 1$, $N_b = 15$.

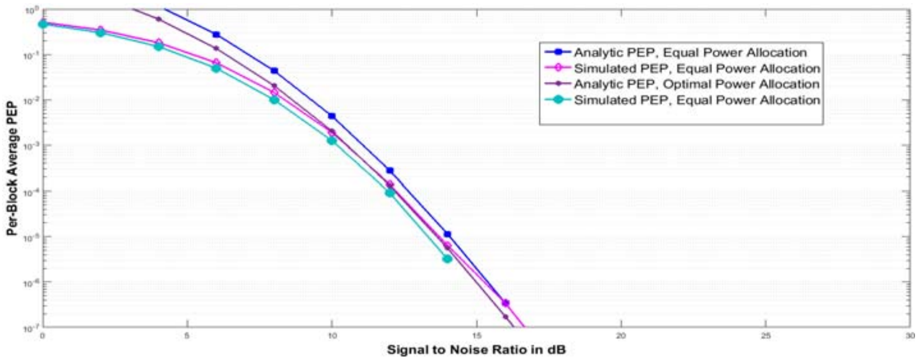

Fig. 4. Per-block average PEP versus SNR in dB for Conventional multiple hop S-DF protocol with optimal power allocation, simulation parameters are $\delta_{SD}^2 = 1$, $\delta_{SR}^2 = 10$, $\delta_{RD}^2 = 50$, $\sigma_{\epsilon_i} = 0.01$, $\sigma_{e_i} = 0.10$, $L = 2$, $\nu = 0.9724$, $N_0 = 1$, $N_b = 15$, $\beta_0 = 0.41$, $\beta_1 = 0.279$, $\beta_2 = 0.32$.

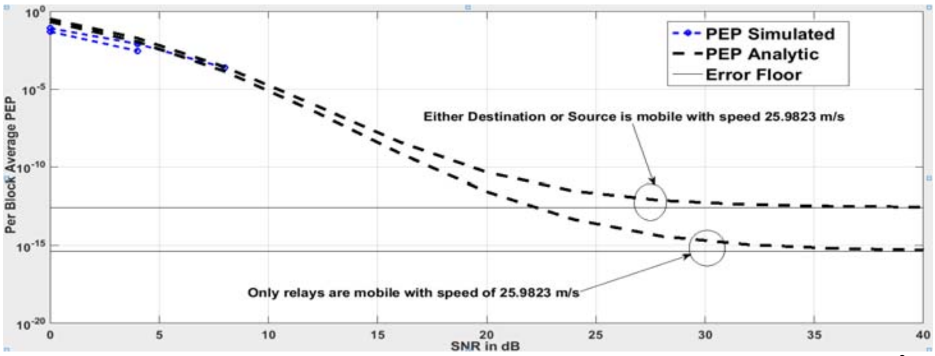

Fig. 5. Per-block average PEP versus SNR in dB of conventional multiple hop protocol with $\delta_{SD}^2 = 10$, $\delta_{SR}^2 = 1$, $\delta_{RD}^2 = 1$, $\sigma_{\in_i} = 0.01$, $\sigma_{e_i} = 0.10$, $L = 2$, $\nu = 0.9723$, $N_0 = 1$, $N_b = 10$.

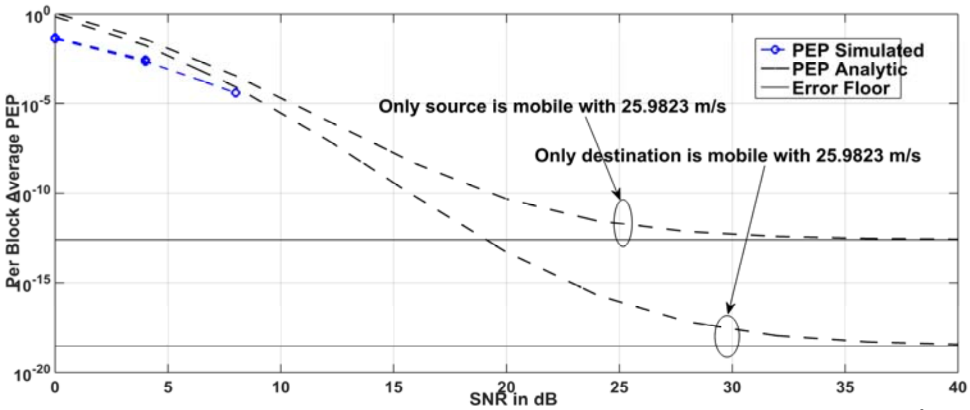

Fig. 6. Per-frame average PEP versus SNR in dB of conventional multiple hop protocol with $\delta_{SD}^2 = 10$, $\delta_{SR}^2 = 1$, $\delta_{RD}^2 = 10$, $\sigma_{\in_i} = 0.01$, $\sigma_{e_i} = 0.10$, $L = 2$, $\nu = 0.9723$, $N_0 = 1$, $M_b = 10$.

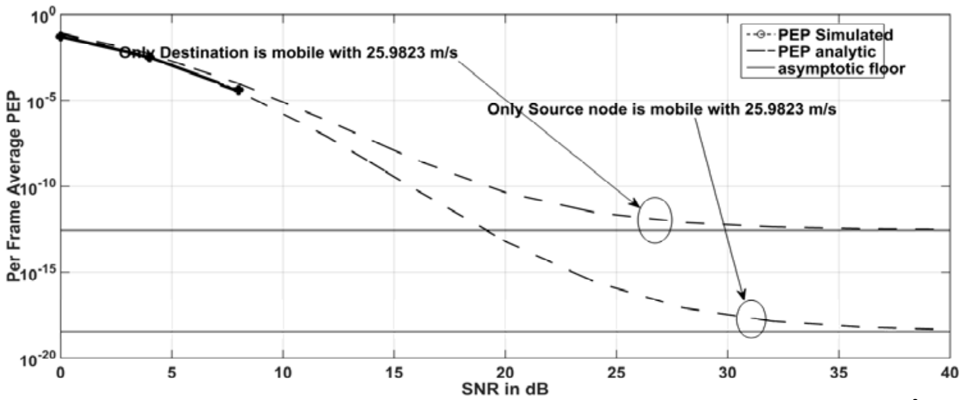

Fig. 7. Per-block average PEP versus SNR in dB of conventional multiple hop protocol with $\delta_{SD}^2 = 10$, $\delta_{SR}^2 = 10$, $\delta_{RD}^2 = 1$, $\sigma_{\in_i} = 0.01$, $\sigma_{e_i} = 0.10$, $L = 2$, $\nu = 0.9723$, $N_0 = 1$, $M_b = 10$.

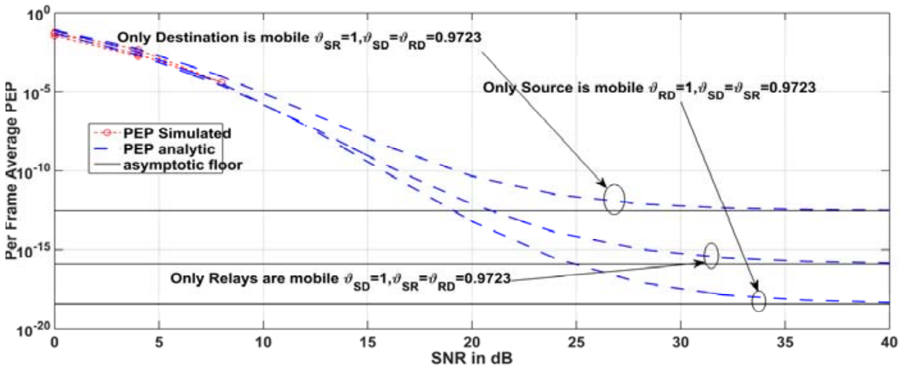

Fig. 8. Per-block average PEP versus SNR in dB of conventional S-DF protocol with $\delta_{SD}^2 = 10$, $\delta_{SR}^2 = 1$, $\delta_{RD}^2 = 1$, $\sigma_{\in_i} = 0$, $\sigma_{e_i} = 0.10$, $L = 2$, $\nu = 0.9723$, $N_0 = 1$, $M_b = 10$.

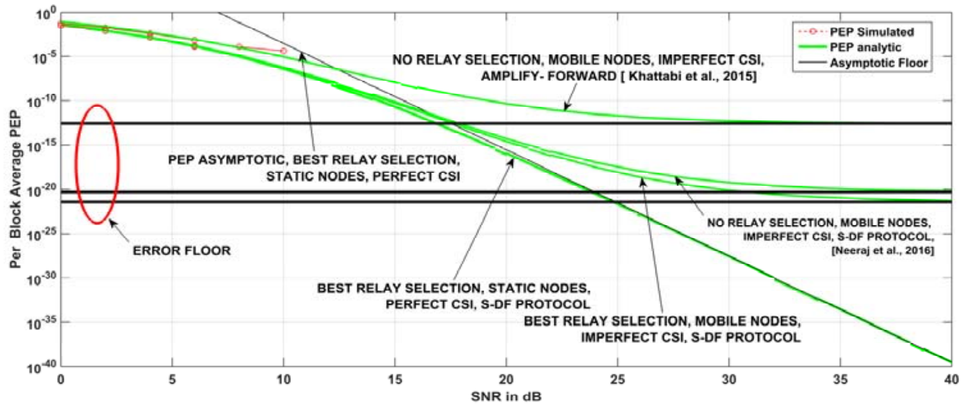

Fig. 9. Comparison between BRS based S-DF, conventional S-DF and AF protocol with $\delta_{SD}^2 = \delta_{SR}^2 = \delta_{RD}^2 = 10$, $\nu = 0.9723$, $M_b = 10$, $L = 2$.

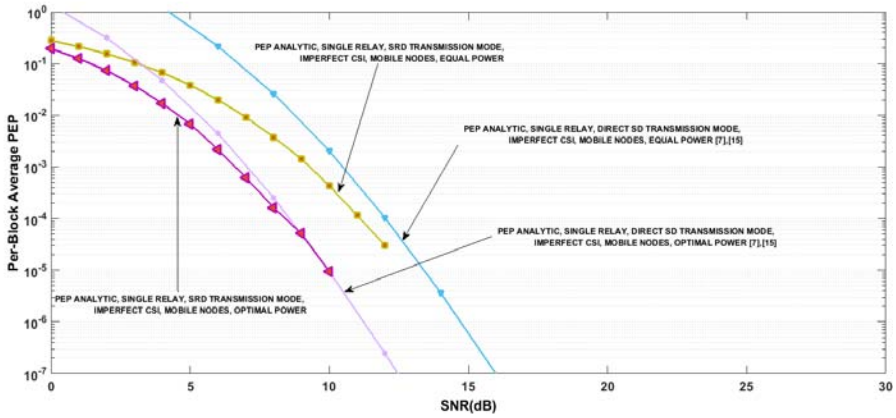

Fig. 10. Comparison between path selection based SRD transmission and Direct SD transmission mode protocol for equal and optimal power, simulation parameters are $a_0 = 0.7052$, $a_1 = 0.30$, $\delta_{SD}^2 = \delta_{SR}^2 = \delta_{RD}^2 = 15$, $\nu = 0.9723$, $M_b = 15$, $L = 2$.

very high. However, when the SR link gain is high as compared to an RD link variance, we get $\beta_0 = \beta_1 = \beta_2 = 1/3$. That is, equal power allocation is the only possible optimal solution. Further, it can be observed from Figs. 3-4 that the optimal power allocation factors optimize the PEP performance in the lower and medium SNR ranges. But at high SNR conditions the per-block average PEP curve approaches to asymptotic curve that is PEP is tight at high SNR values for both equal power and optimal power allocation scenarios. This happens because the per block average PEP performance at high SNR becomes independent of source and relay powers because of the mobility of nodes and imperfect CSI conditions. Fig. 5 presents that, when SR link is same to RD link, *i.e.*, $\delta_{SR}^2 = \delta_{RD}^2$, per-block average PEP performance when RNs are mobile is better than the PEP performance when the SN is mobile. Since SR and RD links have same channel gain, both DN and SN mobility, for equal velocity, have a similar impact on the per block average PEP performance. However, when the RD link gain is higher than the SR link gain, i.e., $\delta_{RD}^2 \gg \delta_{SR}^2$, shown in Fig. 6, PEP performance when DN is mobile is better than PEP performance when the SN is mobile. However, when the SR link gain is higher than the RD link gain, *i.e.*, $\delta_{SR}^2 \gg \delta_{RD}^2$, PEP performance when the SN is mobile is better than PEP performance when DN is mobile, as displayed in Fig. 7. From Figs. 5 and 6 we can show that there is a slight gap between the simulated per-block average PEP performance and analytic per block PEP performance in the lower SNR values. An analogous development can be observed in papers [7, 14] on the end-to-end performance of orthogonal-STBC based dual hop cooperative communication system. This happens because PEP upper-union bound expression is tight only for higher SNR range. Also, it can be observed that from Fig. 7 that when the SR and RD link gain increases, this performance gap decreases significantly. Fig. 8 demonstrates that in the case of knowledge of perfect CSI and when only RNs are moving, the system performance does not experience the error floor limit and DO is equal to $NN_D = 4$. It is significant to the node that system performance of the cooperation network employing S-DF protocol experiences error floor limit. In Figs. 9-10 we compare the per block average PEP performance of the BRS based S-DF protocol and the conventional S-DF and AF protocol over the time varying channel with imperfect CSI and node mobility conditions. In the case of immobile nodes, both relaying schemes do not experience asymptotic error floors limits because of the mobility effect is removed. It can be observed that, in this case, the BRS based S-DF protocol's performance outperforms that of the conventional S-DF and AF protocol at low as well as high SNR regimes. Also, it can be observed from Figs. 9-10 that in case when the SN and the DN are not moving (only RNs are moving), the PEP performance does not experience asymptotic limits.

7. CONCLUSIONS

We investigate the PEP performance for BRS based S-DF protocol over time varying fading channel conditions. The closed form PEP expressions are derived for several configurations in terms of number of hops, phases, and relays over Time selective Rayleigh fading channel, with BRS. Further, a framework is developed for deriving the DO and optimal power allocation factors for each configuration. Simulations have been performed to verify the derived analytical results.

REFERENCES

1. C. R. Sheu, Y.-W. P. Hong, and Y.-S. Wang, "Cooperative communication method and system," *U.S. Patent Application 15/447, 364*, filed May 3, 2018.
2. T. S. El-Bawab, R. Subrahmanyan, G. Atkin, and M. Dohler, "Key technology for 5G new radio," *IEEE Communications Magazine*, Vol. 56, 2018, pp. 1-2.
3. X. H. Ge, "Joint optimization of computation and communication power in multi-user massive MIMO systems," *IEEE Transactions on Wireless Communications*, Vol. 17, 2018, pp. 4051-4063.
4. Z. Hadzi-Velkov, D. S. Michalopoulos, G. K. Karagiannidis, and R. Schober, "On the effect of outdated channel estimation in variable gain relaying: Error performance and PAPR," in *Proceedings of IEEE Transactions on Wireless Communications*, Vol. 12, 2013, pp. 1084-1097.
5. M. R. Avendi and H. H. Nguyen, "Performance of differential amplify-and-forward relaying in multinode wireless communications," *IEEE Transactions on Vehicular Technology*, Vol. 62, 2013, pp. 3603-3613.
6. E. Sanli, F. Kara, and H. Kaya, "Effect of the error propagation on the error performance of cooperative communications with the best relay selection schemes," in *Proceedings of the 26th IEEE Signal Processing and Communications Applications Conference*, 2018, pp. 1-4.
7. Y. M. Khattabi and M. M. Matalgah, "Alamouti-OSTBC wireless cooperative networks with mobile nodes and imperfect CSI estimation," *IEEE Transactions on Vehicular Technology*, Vol. 67, 2018, pp. 3447-3456.
8. C. M. K. Swain and S. Das, "Study and impact of relay selection schemes on performance of an IEEE 802.16 j mobile multihop relay (MMR) WiMAX network," in *Progress in Intelligent Computing Techniques: Theory*, *Practice*, *and Applications*, Springer, Singapore, 2018, 491-499.
9. A. K. Shukla and S. Yadav, "Performance analysis of incremental hybrid decode-amplify-forward cooperative relaying with an opportunistic relay selection under Rayleigh fading channels," in *Proceedings of International Conference on Wireless Communications*, *Signal Processing and Networking*, 2017, pp. 1728-1733.
10. N. Varshney and A. K. Jagannatham, "A unified framework for the analysis of path selection based DF cooperation in wireless systems," in *Proceedings of IEEE Wireless Communications and Networking Conference*, 2017, pp. 1-6.
11. V. S. Krishna and M. R. Bhatnagar, "A joint antenna and path selection technique in single-relay-based DF cooperative MIMO networks," *IEEE Transactions on Vehicular Technology*, Vol. 65, 2016, pp. 1340-1353.
12. M. R. Bhatnagar, R. K. Mallik, and O. Tirkkonen, "Performance evaluation of best-path selection in a multihop decode-and-forward cooperative system," *IEEE Transactions on Vehicular Technology*, Vol. 65, 2016, pp. 2722-2728.
13. L. R. Lakshmi, "Link quality based path selection methods for IEEE 802.16 j mobile multihop relay networks," *Wireless Personal Communications*, Vol. 75, 2014, pp. 579-592.
14. N. Varshney and A. K. Jagannatham, "Outage analysis for path selection based MIMO-beamforming cooperative wireless systems with node mobility and imperfect

CSI," in *Proceedings of International Conference on Signal Processing and Communications*, 2016, pp. 1-5.
15. N. Varshney and A. K. Jagannatham, "MIMO-STBC based multiple relay cooperative communication over time-selective Rayleigh fading links with imperfect channel estimates," *IEEE Transactions on Vehicular Technology*, Vol. 66, 2017, pp. 6009-6025.
16. N. Varshney and A. K. Jagannatham, "Performance analysis of MIMO-OSTBC based selective DF cooperative wireless system with node mobility and channel estimation errors," in *Proceedings of the 22nd National Conference on Communication*, 2016, pp. 1-6.
17. N. Varshney, A. V. Krishna, and A. K. Jagannatham, "Selective DF protocol for MIMO STBC based single/multiple relay cooperative communication: End-to-end performance and optimal power allocation," in *Proceedings of IEEE Transactions on Communications*, Vol. 63, 2015, pp. 2458-2474.
18. N. Varshney, A. V. Krishna, and A. K. Jagannatham, "Capacity analysis for path selection based DF MIMO-OSTBC cooperative wireless systems," *IEEE Communications Letters*, Vol. 18, 2014, pp. 1971-1974.
19. N. Varshney and P. Puri, "Performance analysis of decode-and-forward-based mixed MIMO-RF/FSO cooperative systems with source mobility and imperfect CSI," Journal of Lightwave Technology, Vol. 35, 2017, pp. 2070-2077.
20. K. J. R. Liu, A. K. Sadek, W. Su, and A. Kwasinski, *Cooperative Communications and Networking*, Cambridge University Press, UK, 2009.
21. C. Chi, W. Li, and C. Lin, *Convex Optimization for Signal Processing and Communications: From Fundamentals to Applications*, CRC Press, FL, 2017,

Ravi Shankar received the M.Tech. degree in Electronic Engineering from GGSIP University, New Delhi in 2012. Since 2015 he is currently pursuing the Ph.D. degree in the Department of Electronic and Computer Engineering, National Institute of Technology Patna, India. His research interests include wireless sensor networks, cooperative communication, MIMO and communication networks.

R. K. Mishra received the M.Tech. degree in Electronic Engineering from University of Burdwan in 2004. He did his Ph.D. degree in the Department of Electronic and Computer Engineering, LNM University, India in 2011. Currently he is working as an Assistant Professor in NIT Patna, India. His research interests include wireless sensor networks and communication networks.